UNIVERSITY OF CALIFORNIA, SAN DIEGO

Characterization of a Naturally Derived Cardiac Extracellular Matrix Hydrogel

A Thesis submitted in partial satisfaction of the requirements for

the degree Master of Science

in

Bioengineering

by

Stephen YuHsiang Lin

Committee in charge:

Professor Karen L. Christman, Chair
Professor Adam Engler
Professor Shyni Varghese

2012

Signature Page

The Thesis of Stephen YuHsiang Lin is approved, and it is acceptable in quality and form for publication on microfilm and electronically:

_____

_____

_____
Chair

University of California, San Diego

2012

DEDICATION

This thesis is dedicated to my family and friends who believed in me every step of the way.

TABLE OF CONTENTS

LIST OF FIGURES

LIST OF TABLES

LIST OF GRAPHS

ACKNOWLEDGEMENTS

I would first like to acknowledge Dr. Karen L. Christman for her guidance and support over the years. She has provided valuable guidance and without her help, this thesis would not have been possible.

I would also like to thank my lab mates for their support and assistance throughout the years. I would especially like to thank Jessica DeQuach for her guidance and thoughtful input with my experiments and projects. I would also like to acknowledge Todd Johnson for being a valuable collaborator in characterizing the extracellular matrix material.

Chapter 2, in part, is a reprint of material that is published as: Johnson TD, Lin SY, Christman KL (2011) Tailoring material properties of a nanofibrous extracellular matrix derived hydrogel. Nanotechnology 22: 494015

ABSTRACT OF THE THESIS

Characterization of a Naturally Derived Cardiac Extracellular Matrix Gel

by

Stephen YuHsiang Lin

Master of Science in Bioengineering

University of California, San Diego, 2012

Professor Karen L. Christman, Chair

The extracellular matrix (ECM) is a complex composition of proteins, proteoglycans, and glycosaminoglycans. Biological scaffolds composed of ECM have been used to help repair a variety of tissues in the body. It has been shown that an extracellular matrix material can be generated by decellularizing cardiac tissue and processed into injectable formulations for cardiac tissue engineering. When brought to physiological conditions, the matrix material will self-assemble into a porous hydrogel. The objective of the present study is to prepare the gel form of the myocardial matrix, characterize and tailor material properties of the gel, compare material properties to a human derived myocardial matrix gel, and finally evaluate the ability of the gel to

support the growth of smooth muscle cells *in vitro*. Material properties including viscosity, swelling ratio, gelation kinetics, and stiffness were assessed.

The results of the study show that material properties of the myocardial matrix can be tailored by adjusting gelation conditions. Changes in final pH, salt concentration, and protein concentration had effects on viscosity and gelation kinetics but not swelling ratio. This study also shows that there are differences in material properties between that of the porcine myocardial matrix and the human myocardial matrix. Finally the study demonstrated that myocardial matrix supported the adhesion and proliferation of rat aortic smooth muscle cells under static conditions.

CHAPTER ONE:

INTRODUCTION

1.1 Myocardial Infarction and Heart Failure

Cardiovascular disease is the leading cause of death in the western world with heart failure following myocardial infarction being major contributor of these deaths. Approximately 785,000 people in the United States suffer from a new myocardial infarction, and about 470,000 people suffer from recurrent attacks each year. In addition, 5.7 million people suffer heart failure, with approximately 670,000 new cases reported annually [1].

A myocardial infarction occurs when blood flow is critically reduced to a region of the heart due to the occlusion of a coronary artery. If the resulting ischemia is of significant duration, the oxygen shortage impairs regular cellular metabolism and leads to injury of the myocardial tissue. In humans, cardiac myocytes have very limited proliferative capabilities post-MI so regeneration is very limited[2]. The necrotic tissue is replaced by collagenous scar tissue [3]. With the loss of contractile tissue, in conjunction with the stiff scar tissue, the rest of the heart tries to compensate for the loss of cardiac output. As a result, the heart goes through a series of compensatory changes including hypertrophy of viable myocytes and dilation of the left ventricle [4,5], which ultimately leads to heart failure and death.

Immediately after a myocardial infarction, myocyte death and the release of cellular contents trigger the inflammatory response. During the early stages of the inflammatory response, macrophages, monocytes neutrophils are recruited to site of injury [6,7]. These cells release matrix metalloproteinase (MMP) which are responsible

for degrading the extracellular matrix. This degradation of the extracellular matrix causes myocytes to slip away and leads to widening of the infarct region.

After the initial inflammatory response, fibroblasts and myofibroblasts quickly proliferate and begin to produce matrix macromolecules, predominantly collagen types I and III. The newly deposited collagen begins as an immature form that consists mostly of the thin collagen type III. As the collagen matures, it develops intermolecular cross links, losses of water, and the thin collagen III is replaced by collagen type I [7]. This results in a stiff scar tissue that is resistant to distention.

The presence of this stiff scar tissue along with the loss of contractile tissue causes several negative changes to the heart. Neighboring healthy tissue dilates to preserve stroke volume which increases stress in the heart wall [8]. The healthy myocytes also undergo hypertrophy in attempts to make up for the loss of contractile tissue[9] and this negative ventricular remodeling leads to increased risk of heart failure and death [10].

As myocardial infarction and the ensuing heart failure continue to be a leading cause of death, it is evident that new therapies need to be developed to slow the rate of deaths.

1.2 Current Clinical Treatments

The only successful treatment for end-stage heart failure currently available is total heart transplantation. However, the shortage of donor organs and strict exclusion criteria limit the availability of this treatment. With only about 2,000 total heart

transplant operations done annually [11], it is unable to meet the demands of the approximately 5.7 million people in the Unites States suffer from heart failure.

Other therapies for myocardial infarctions are available but they aimed at reducing damage and do not promote healing. For patients suffering from acute myocardial infarction that are given immediate medical care, current medical guidelines recommend urgent reperfusion through the use of thrombolytic therapy (fibrinolysis) [12-15]. In this procedure, the patient is given anticoagulant drugs such as aspirin, tissue plasminogen activator (t-PA), or streptokinase (SK) to dissolve blood clots that may have caused the occlusion of the coronary artery [16]. The use of beta blockers has also been shown to reduce the magnitude of infarction and increase survival[17]. If a catheter lab is available, surgical interventions such as angioplasty, stenting and bypass surgery have also been recommended for the rapid reperfusion of the blocked artery [18]. These rapid reperfusion therapies aim to reduce the time of ischemia in hopes of limiting infarction and necrosis of the heart.

Several pharmacological agents are prescribed to treat heart failure. These include diuretics, angiotensin converting enzyme (ACE) inhibitors, digitalis, and beta blockers[19]. The diuretics work by preventing fluid accumulation in the body. ACE inhibitors are used as a vasodilator to reduce blood pressure and reduce work load on the heart. Digitalis glycosides are inotropic agents that increase the strength of the contractions of the heart muscle and help reduce heart failure symptoms. Beta blockers reduce heart rate and blood pressure.

Besides the use of pharmacological agents, left ventricular assist devices (LVADs) have been used to treat heart failure. LVADs are pumps attached to the left ventricle and the aorta and help pump blood to the rest of the body. The pump is powered by an external battery pack. Although the LVADs do restore blood flow to the body, they increase the risk of infection, internal bleeding, and pump failure[20], and also promotes cardiac disuse atrophy[21].

With heart transplantation being limited by the number of donor organs available and limitations with the use of LVADs and medication, there is a pressing need to develop alternative treatments.

1.3 Biomaterials for the Treatment of MI

The development of biomaterials has become a major research focus as a promising alternative therapy for myocardial infarction. These biomaterials are designed to replace the damaged extracellular matrix of the heart in attempts to retain structural integrity, to regenerate the necrotic tissue, and prevent heart failure.

Three main approaches have been investigated the delivery of biomaterials for the treatment of myocardial infarction. One approach is the use of ventricular restraints that are applied around the heart via open heart surgery to prevent heart failure. A second approach is to generate biomaterial scaffold patches *in vitro* and implant them onto the heart. The last method is to inject the biomaterial into the heart and form the scaffold *in situ*.

Left ventricular restraints were one of the first approaches investigated for the treatment of heart failure. In this approach, polymer meshes were placed around the

heart to prevent it from enlarging during ventricular remodeling. Some examples of these meshes include poly(propylene) and polyester. Several studies have shown improved ejection fraction and decreased LV end-diastolic volume.

More recently, biomaterials have been designed as cardiac patches to be applied to the surface of the heart as scaffolds. These scaffolds can be made out of a wide variety of materials such as gelatin, poly(glycolide)/poly(lactide), collagen, alginate, or matrigel. They are applied to the heart as acellular scaffolds, with cell, or with growth factors. When applied with cells, some studies have shown vascularization of the scaffold and survival of the cells. In addition, there has been evidence that the patches prevent infarct wall thinning and also improved fractional shortening.

Injectable biomaterial scaffolds are materials that have been specifically engineered to gel *in situ.* Like the previously mentioned cardiac patches, injectable scaffolds can also be delivered as acellular scaffolds, with cell therapies, or with growth factors. This strategy is extremely promising because it prevents an invasive open chest procedure required for the application of the cardiac patches and restraints.

1.3.1 Synthetic Materials

There are two main approaches to developing biomaterials for cardiac repair applications. First is to design the material using synthetic materials to chemically synthesize the biomaterial. The second approach is to harvest materials from biological sources and process them into their final usable formulations.

Synthetic materials offer the advantage of precise control over important material properties such as degradation rate, swelling ratio, stiffness, and porosity[22].

They also do not face the problem of batch-to-batch variability seen in naturally derived materials. Polyester, polyurethane, poly(ethylene glycol)(PEG), and poly(Nisopropylacrylamide) (PNIPAAM) are examples of recently developed materials that have shown promise in the treatment of MI.

Polyester meshes have been designed as LV restraints that are fitted around a heart post-MI to preserve the geometry of the heart during negative LV remodeling. Results showed that the LV restraint device reduced myocyte hypertrophy, LV end-diastolic volume, and interstitial fibrosis. It also increased fractional shortening [23].

PNIPAAM is a thermo-responsive hydrogel that remains in a liquid state at room temperature but forms a hydrogel at 37 ºC. It has been modified with other monomers such as acrylic acid (AAc) and hydroxyethyl methacrylate-poly(trimethylene carbonate) (HEMAPTMC) to form poly(NIPAAm-co-AAc-co-HEMAPTMC). When injected in a rat infarct model, it prevented ventricular dilation and improved contractile function[24]. Other variations of PNIPAAM, such as Dex-PCL-HEMA/PNIPAAm, have also shown improvements in left ventricle ejection fraction and the prevention of LV remodeling and dilation when injected 4 days post-PI in a rabbit ischemia model[25].

PEG is another material that has been extensively explored for potential in treatment for MI. It was once thought that the increase of wall thickness at the site of infarction alone could increase cardiac function by decreasing wall stress. However, studies have shown the direct injection of non-degradable PEG into the infarct region 1 week post-MI in a rat ischemia model showed no improvement in cardiac function 7

weeks post-MI[26]. This suggests that in addition to mechanical support, biomaterials must also have proper biochemical cues to direct cardiac regeneration.

Although synthetic materials have shown promise, they lack the inherent bioactivity which may be important in directing cellular behavior and cardiac regeneration.

1.3.2 Naturally Derived Materials

Naturally derived materials have been explored to treat the heart post-MI because they offer the advantage of being intrinsically biocompatible and are degraded into safe byproducts[27]. Collagen, being the predominant protein in the extracellular matrix, is one of the first biomaterials explored to be used as a scaffold for cardiac tissue engineering[28] . In a rat cryoinjury model, the application of a porous collagen scaffold implanted on the intact heart and showed increased levels of angiogenesis [29]. Another study showed that injection of collagen into the left ventricle in a rat model preserves cardiac function after myocardial infarction[30].

The use of fibrin glue has also shown beneficial effects when injected into the myocardium. Fibrin glue is injected as a two component system, consisting of fibrinogen and thrombin. Upon mixing, thrombin converts fibrinogen into fibrin, a fibrous protein involved in the clotting of blood, to create a fibrin gel. The fibrin glue is known to promote angiogenesis. The fibrin glue has been shown to preserve infarct wall thickness and cardiac function[31].

Alginate is another naturally derived material that has shown positive results when used as a scaffold for cardiac tissue engineering. Alginate is a polysaccharide that is derived from seaweed and will form a gel using calcium present in cardiac tissue. When injected into the myocardium one week most-MI, it showed increased scar thickness, and improved left ventricular ejection fraction[32]. It has also shown improvement in cardiac function in a porcine model while utilizing a minimally invasive delivery technique [33].

Another interesting material that has shown promising results is Matrigel. Matrigel is a purified matrix that is derived from a mouse sarcoma cell line. It is comprised of a complex mixture of extracellular components including collagen, laminin, entactin, and heparin sulfate. In addition, it self assembles into a hydrogel when brought to 37C. Injection of Matrigel immediately post-MI led to increased infarct wall thickness, neovascularization and improved ejection fraction [34]. However, Matrigel is derived from a cancerous cell line, and has been shown to support cancerous growths in vitro and in vivo [35] and will limit its ability to be clinically translatable.

However, material properties of naturally derived materials are difficult to control and must be carefully characterized to better understand the behavior of the material.

1.3.3 Decellularized Extracellular Matrix

In addition to the previously described naturally derived materials, there has been recent development in decellularized materials. Decellularized materials are promising because they take advantage of nature's platform to create an intrinsically complex extracellular matrix scaffold that is thought to better mimic the native extracellular environment. The processing of decellularized ECM begins with tissue, where the tissue is stripped of all cellular components through physical, chemical, or enzymatic processing[36]. The final product can then be used either as cardiac patches or further processed into injectable scaffolds that form gels *in situ* or injectable emulsions[10,37].

Some examples of these decellularized ECM materials include small intestine submucosa (SIS) ECM, urinary bladder matrix (UBM)[38], and myocardial matrix[10]. Urinary bladder matrix has been used as a cardiac patch in a pig infarct model and showed cellular infiltration and neovascularization into the patch[39].

SIS ECM has also been shown to be beneficial in a rat ischemia-reperfusion model. The SIS ECM was processed into a powder and rehydrated as a suspension. The emulsion was then injected into the rat myocardium at different time points post-MI. The results showed that the SIS ECM enhanced cellular infiltration and angiogenesis when compared to the control. It also showed improvements in cardiac function when compared to the saline control [40].

Perhaps, a more promising material for cardiac repair is the extracellular matrix material derived from the healthy myocardium. Because it is derived from the very

tissue it is meant to replace, it contains a tissue specific combination of proteins and proteoglycans. The material has shown promise for the use in cardiac repair, which will be further discussed in section 1.5.

1.4 Cellular Delivery with Biomaterials

Cell therapies have been explored as a potential treatment to repair the necrotic tissue of the heart after a myocardial infarction. Early attempts to transplant cells into the injured myocardium post-MI used cells suspended in an aqueous solution. These transplantations had only limited success because of limited cell retention and transplant survival. Studies have shown ~90% of cells delivered to the heart are lost to circulation or leak out of the injection site [41]. Furthermore, ~90% of the successfully delivered cells die within the first week. This may be in-part be due to the non-ideal conditions of an ischemic region and the fact that the injected cells do not have a place to attach to. To solve these problems, injectable scaffolds that gel *in situ* have been combined with cellular delivery for cardiac repair.

The fibrin glue system described in section 1.3.2 is one of the injectable scaffolds that have been combined with cells for injection. The injection of fibrin with skeletal myoblasts has shown preservation of cardiac function and infarct wall thickness. Bone marrow mononuclear cells have also been combined with fibrin and enhanced neovascularization in infarcted myocardium[31,42].

Chitosan is another material that gels *in situ* that has been explored cellular delivery. Chitosan is a polysaccharide derived from crustacean shells that can be designed to undergo temperature-phase transitions at 37ºC. When injected with mouse

embryonic stem cells into an infarcted myocardium, it preserves cardiac function and myocardial wall thickness, and enhances angiogenesis [43].

1.5 The Cardiac Extracellular Matrix

The injectable form of myocardial extracellular matrix is a biomaterial developed in the Christman lab. In brief, the left ventricle from a porcine heart is processed by decellularization using sodium dodecyl sulfate, lyophilization, mechanical milling, followed by pepsin enzymatic digestion to yield a liquid form of the myocardial extracellular matrix. The matrix can then be brought to physiological conditions of pH 7.4, 1 x salt concentration and 37ºC to form a hydrogel[10]. This myocardial extracellular matrix has a complex composition with an abundance of different extracellular matrix proteins, proteoglycans, and glycosaminoglycans. There have been multiple studies that show the beneficial use of this material in both *in vitro* and *in vivo* applications with the hypothesis that the complex composition would provide a better representation of the *in vivo* microenvironment.

Singelyn et al. demonstrated that vascular cells migrate towards the solubilized myocardial matrix significantly more than collagen, FBS or pepsin *in vitro*. This strongly suggested the material has the potential for vascular formation. In the same study, the myocardial matrix was injected into the left ventricle of healthy Sprague-Dawley rats to. 11 days post-injection, endothelial cells and smooth muscle cells infiltrated the material and arteriole formation was observed[39]. In another *in vivo* study, Singelyn et al showed that cardiac function is preserved in a rat ischemia-

reperfusion model when myocardial matrix is injected into the heart wall post-MI[44]. This confirms the potential for the material to be injected as an acellular therapy for MI.

In addition, Singelyn et al. further demonstrated that the material properties of the myocardial matrix can be modified through the use of the chemical cross-linker, glutaraldehyde. It was shown that after cross-linking, the material showed increased stiffness, slowed cellular infiltration, and decreased material degradation. Thus, it was demonstrated that the myocardial matrix has potential to be further modified to fit other tissue engineering requirements[45].

DeQuach et al. showed that the myocardial matrix could be used in its solubilized form as a tissue specific cell culture coating. When human embryonic stem cell derived cardiomyocytes were seeded on the myocardial matrix coating, the cells showed a significant increase in maturation compared to a standard gelatin coating[46]. Thus, suggesting that the myocardial matrix material may be beneficial as a platform in conjunction with cellular therapies to enhance maturation of cardiac-relevant cell types.

1.6 Objectives

The purpose of this thesis was to further study the gel form of the myocardial extracellular matrix that has shown potential as an injectable scaffold for the treatment of myocardial infarction. The porcine myocardial extracellular matrix hydrogel was further characterized for material properties including gelation kinetics, storage modulus, and swelling ratio. A subset of these properties was shown to be modulated when gelation conditions were altered. In addition, a human myocardial extracellular

matrix hydrogel was also characterized for the same material properties, which could be a potential allogeneic source of the material. Finally, the *in vitro* feasibility of the porcine myocardial matrix hydrogel was investigated.

In addition to providing proper biological and chemical cues, the mechanical properties of tissue engineering scaffolds must also be considered, as it is known that a material's mechanical properties have been shown to influence and direct cell behavior. Thus, one of the goals of this study was to investigate different methods to tailor the mechanical properties of an already developed extracellular matrix scaffold. The important mechanical properties such as swelling ratio, viscosity, and gelation time have not been previously examined. Although the ideal mechanical properties for cardiac regeneration have not been well defined, further characterizing the properties of the porcine myocardial matrix and the understanding how to modulate them is important for future tissue engineering applications.

Tissue from an allogeneic source was also characterized in this study. As the human myocardial tissue was found to contain fat, a further processing step was needed as isopropanol was used to dissolve out the lipids. However, the addition of isopropanol may have affected the final decellularized product in unknown ways. Therefore, another goal of the study was to determine the effects of isopropanol on material properties, and also compare the material properties of human myocardial matrix to porcine myocardial matrix.

The culturing of cells on a collagen I hydrogel scaffolds has been investigated previously and have been shown to support cell adhesion and proliferation[47]. In

addition, it was previously shown that the myocardial matrix encourages the maturation of cardiomyocytes when used as a 2D coating. Therefore, we sought to determine if the myocardial matrix in a hydrogel form can be used as a model to study cellular behavior. As a result, the study aimed to examine the cytocompatibility of the myocardial matrix gel form *in vitro*.

CHAPTER TWO:

MATERIAL CHARACTERISTICS OF A NATURALLY DERIVED CARDIAC EXTRACELLULAR MATRIX HYDROGEL

2.1 Introduction

The myocardial matrix is a tissue specific injectable scaffold designed for cardiac tissue engineering applications. Derived from the native myocardium, it uses nature's platform to retain chemical and biochemical cues essential. It consists of a complex mixture of extracellular matrix proteins, proteoglycans, and glycosaminoglycans, which is thought to mimic the cell's native environment. Studies have shown that interactions between the cell and the extracellular environment are essential for controlling cell migration, proliferation, differentiation, mechanical stability, and signaling[48-50].

In addition to having the appropriate biological and chemical cues, mechanical properties is another important parameter to consider when designing a scaffold for tissue engineering applications. Studies have shown the importance of mechanical properties on cell-matrix interactions and cell behavior. Previously, the effect of chemical crosslinking using glutaraldehyde on the myocardial matrix has been investigated [45]. It was shown to increase stiffness, decrease degradation, and slow cell migration. However, other important material parameters such as viscosity, gelation kinetics and swelling ratio have not been previously studied. In addition, altering the gelation conditions of pH and salt concentration and its effect on these material characteristics has not been studied.

When considering a material for injectability, the viscosity of the liquid form and the speed of gelation are important parameter to understand. The viscosity must be

low enough to allow for the material to pass through the catheter without too much resistance.

Of the extracellular matrix proteins, collagen is the most prominent and best characterized component. Collagen is a fibrous protein with a core triple helical structure. Collagen can be similarly processed into an injectable solubilized form, which can self-assemble into a hydrogel under certain conditions [51,52]. Effects of varying ion concentration, phosphate concentration, and pH and material concentration on collagen gel behavior have been previously described [53,54] [55]. As a result, these parameters were altered to determine the how the myocardial matrix responds.

In addition to measuring the changes of the porcine myocardial matrix, the material properties of a human myocardial matrix were also determined. During the initial decellularization of the human myocardium, it was observed that the tissue had considerably more fatty tissue. As a result, an extra step using 100% isopropanol was added to dissolve out the fat. However, the isopropanol also washes out other unknown components of the material and affects the final decellularized product. Therefore another goal of the study was to compare the different processing protocols on material properties of human myocardial matrix, and also compare human myocardial matrix to porcine myocardial matrix.

The present study characterizes the ECM materials by using rheometry to determine stiffness and viscosity, spectrophotometry to assess gelation kinetics, and a mass ratio to determine swelling ratio.

2.2 Materials and Methods

2.2.1 Decellularization of Porcine Tissue

Porcine myocardial tissue was harvested and decellularized following a modified version of a previously established protocol[10]. Porcine hearts were harvested from Yorkshire pigs, approximately 30-45kg. The left ventricle was extracted and trimmed of fat and connective tissue. The tissue was then sliced into small pieces and rinsed with deionized water for 30 minutes then decellularized in a solution of 1% (wt/vol) sodium dodecyl sulfate (SDS), phosphate buffered saline (PBS), and 0.5% Penicillin/Streptomycin for 4-5 days with solution changes every 24 hours. Once decellularized, the tissue was stirred in 0.01%(vol/vol) Triton X-100 for 30-45 minutes followed by deionized water for 24 hours to ensure removal of residual SDS. The tissue was then frozen at -80C, lyophilized and milled using a Wiley Mini Mill to create a fine powder

2.2.2 Decellularization of Human Tissue

Human hearts from non-cardiac related deaths were received, through collaboration with the Mayo Clinic. The human myocardial tissue was decellularized using a method similar to the decellularization of porcine myocardial tissue. In short, the hearts were trimmed of fat, connective tissue and major vessels and cut into small pieces and rinsed with deionized water for 30 minutes followed by decellularization in a solution of 1% (wt/vol) sodium dodecyl sulfate (SDS), phosphate buffered saline (PBS),

and 0.5% Penicillin/Streptomycin for 4-5 days with solution changes every 24 hours. After the material and the SDS solution no longer had color, the material was treated in one of two methods. The first, which is termed “standard” was processed the same way as the porcine myocardial matrix. The second, which is termed “IPA” was stirred in 100% isopropanol for 24 hours to remove lipids[56], rehydrated in water for 24 hours. Both sets were then stirred in 0.01 % Triton X-100 for 1 hour to remove residual SDS. The tissue was then frozen at -80C, lyophilized and milled using a Wiley Mini Mill to create a fine powder

2.2.3 ECM Digestion and Gelation

The porcine extracellular matrix material was enzymatically digested by adding a 1 mg ml−1 solution of pepsin (Sigma, St Louis, MO) in 0.1 M HCl such that the final concentration of material was 10 mg ml−1[10,57]. The material was digested for 48– 60 hours at room temperature with constant stirring until the liquid was homogeneous with no visible particles. The pepsin was irreversibly inactivated by raising the pH. The pH (7.4 or 8.5) and salt concentration (0.5×, 1.0×, or 1.5× PBS) was adjusted using 1.0 M NaOH and 10× PBS, respectively, to end with the desired final material concentration (6 or 8 mg/ml). The final mixture was then brought to at 37 ºC and allowed to fully gel. Standard conditions are defined as physiological conditions of pH 7.4, 1.0×PBS, and 37 ºC. Only one parameter (salt concentration or pH) at a time was varied away from these standard conditions for any of the following experiments. The human extracellular

matrix material was prepared in the same manner as the porcine extracellular matrix but with only standard conditions.

2.2.4 Rheometry: Storage Modulus, Loss Modulus

Rheological measurements were made with a TA Instruments ARG2 Rheometer. Modified from a previous method[57], a parallel-plate geometry (20 mm diameter) at 1.2 mm gap height was used on 500 μl gels under the different conditions after 24 h of gelation. For each condition, the storage modulus (*G*') and loss modulus (*G*") over frequencies of 0.04–16 Hz were recorded for every gel condition in triplicate. The storage modulus at 1 rad s−1 or 0.16 Hz was plotted for each condition.

2.2.4 Rheometry: Viscosity

For viscosity, samples were prepared as discussed earlier and kept on ice in the liquid form until experimentation. The rheometer was preheated and maintained at 25 ºC. Then 200 μl of sample was loaded into the rheometer set at 500 μm gap height such that the sample completely filled the gap. Measurements of viscosity were made over a frequency range of 0.1–50 Hz as previously reported. The data were best-fit to the following power law:

$$\eta = kf^n \quad (1)$$

In this equation (η) is the complex viscosity and (f) is frequency, with (k) and (n) being constants.

2.2.5 Swelling Ratio

ECM gels of 250 μl for each condition in triplicate were formed in a 48-well plate for 24 h at 37 ◦C. The gels were transferred to a 12-well plate and were allowed to swell in PBS for 24 h. The samples were removed, carefully blotted to remove excess surface liquid, and the total swelled weight was measured (*W*s). Then the samples were fully dried using a vacuum desiccator overnight and total dry weight was measured (*W*d). Swelling ratios were calculated as:

$$Swelling\ ratio = \frac{W_s - W_d}{W_d}.$$

2.2.6 Turbidimetric Gelation Kinetics

Turbidimetric gelation kinetics was determined through spectrophotometric measurements as previously described. First, a Synergy™ 4 Multi-Mode Microplate Reader (Biotek) was preheated to 37 ºC. Then 100 μl of each ECM sample, prepared as previously described, was placed into a 96-well plate in triplicate. Absorbance was measured at 405 nm wavelength every minute for 8 h or until the data plateaued. Absorbance values were averaged within each group, normalized, and plotted over time. From the normalized plot, a linear fit was applied to the linear region of the plot to calculate the half time of gelation ($t_{1/2}$), the lag phase (t_{lag}), and the slope or speed of gelation (*S*). The half time of gelation was defined as the time when the material reached 50% of the maximum measured absorbance. The lag phase was calculated by finding the time at which the linear fit was zero for normalized absorbance.

2.3 Results

2.3.1 Confirmation of Gelation

Gelation of both the porcine and human extracellular matrix material was first confirmed at standard conditions. The extracellular matrix remained a viscous liquid after neutralization to pH 7.4 while kept at 4°C (Fig 1a). After the extracellular matrix was brought to 37°C to induce gelation, a soft gel was created. Both the porcine and the human extracellular matrix formed a soft gel. The gelation was confirmed by tilting them to the sides and observing that they maintained their shape (fig 1b, fig 1c).

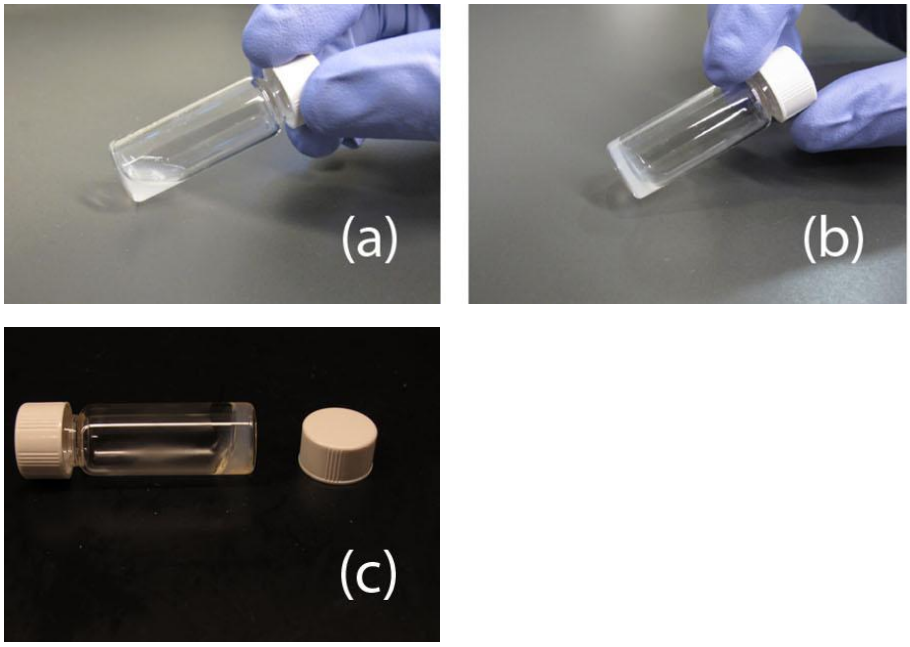

Figure 1: Gelation of myocardial matrix hydrogel. (a) The solubilized from of porcine myocardial matrix; (b) at physiological conditions, the porcine myocardial matrix forms a gel that maintains shape; (c) at physiological conditions, the human myocardial matrix forms a gel that retains its shape

2.3.2 Rheometry: Storage Modulus and the Loss Modulus

Rheometry was used to measure the storage modulus and the loss modulus to determine the differences in material properties between the human and porcine extracellular matrix gels at standard conditions. In addition, the effects of an isopropanol wash on material properties of the human ECM gels were also examined. The values for 6mg/mL gels are represented in Table 1 and values for 8mg/mL gels are represented in Table 2. Increasing material concentration of each material from 6mg/mL to 8 mg/mL significantly increased the storage modulus, indicating the increase of material concentration leads to stiffer gels. The storage modulus of the porcine ECM gels (data courtesy of Todd D. Johnson) was also significantly larger than the human ECM gels when processed in the same manner. When the human ECM was processed with IPA, it led to a significant increase in the storage modulus.

Table 1. Storage modulus (G') and loss modulus (G") of 6mg/mL after 24 h gelation at 37C

Condition	G'(Pa)	G"(Pa)
Porcine Standard	5.28 ± 0.41**	0.893 ± 0.085**
Human Standard	3.48 ± 0.12	0.612 ± 0.095
Human IPA	4.52 ± 0.50	0.92 ± 0.104

Mean ± SD
** Courtesy of Todd D. Johnson[58]

Table 2. Storage modulus (G') and loss modulus (G") of 8mg/mL after 24 h gelation at 37C

Condition	G'(Pa)	G"(Pa)
Porcine Standard	9.52 ± 3.77**	1.75 ± 0.72**
Human Standard	6.30 ± 0.91	1.80 ± 0.18
Human IPA	8.00 ± 1.18	1.22 ± 0.24

Mean ± SD
** Courtesy of Todd D. Johnson[58]

2.3.3 Viscosity

The myocardial matrix has been previously used as an injectable material delivered via catheter. When considering a material for injection, understanding the viscosity of the liquid state is very important to assure proper flow through both the catheter and the needle. The complex viscosity of both the porcine and human myocardial matrix in liquid form at 25ºC was assessed over a range of shear rates. Across all samples, the complex viscosity decreased as the shear rate increased. A linear trend is observed when plotted on a log-log scale. As a result, the power equation was used to fit the data. The reported values of (*k*) and (*n*) are constants from the power equation used to fit the data. The coefficient of determination (r^2) indicates the accuracy of the power equation fit with a value of 1 indicating a perfect fit. When comparing the different gelation conditions for the porcine myocardial matrix, dramatic differences in complex viscosities were only seen between the different protein concentrations. Changes in salt concentration or pH had no effect. Increasing the concentration of the porcine myocardial ECM in the liquid form increased intermolecular forces, resulting in an increase in viscosity. This significant increase in viscosity can be observed as a

vertical shift of the data points in graph 1. This trend is also confirmed by the increase of (k) values between the 6mg/ml and the 8 mg/ml samples.

When comparing the complex viscosities of the liquid human myocardial matrix under different processing procedures, it is seen that the IPA treated material had a slight increase in complex viscosity. The increase can be observed in both the vertical shift of the data points, as well as a difference in the (k) coefficient. The increase in viscosity can be attributed to the IPA removing additional fatty components, leading to a more concentrated end protein mixture. When comparing the human myocardial matrix to the porcine myocardial matrix, the (k) values are very similar.

The (*n*) value correlates to the slope of the fitted line when plotted on a log-log scale. The (n) values for the 6 mg/mL porcine myocardial matrix range from -0.466 to -0.550 and are larger than the 8 mg/mL values, which range from -0.580 to -0.656. This slight variation can be observed in figure X. The (n) values for the two methods of processing the human myocardial matrix are very similar, with a value of -0.572 for standard processing and -0.555 with the additional IPA step. When compared to the human myocardial matrix to the porcine myocardial matrix, the (n) values deviate slightly. The (n) values across all samples are observed to be negative, which indicate that the material is shear thinning. Because of this, the materials will have a lower viscosity when experiencing higher shear rates, such as those that occur when passing through a catheter or needle during injection.

Table 3. Complex viscosity of the liquid porcine myocardial matrix material at 25°C

Condition	*k*	*n*	r^2
6mg/ml			
Standard	0.1300	-0.466	0.955
0.5x PBS	0.1548	-0.523	0.959
1.5x PBS	0.1580	-0.519	0.963
8.5 pH	0.2030	-0.550	0.978
10.0 pH	0.1502	-0.523	0.907
8mg/ml			
Standard	0.4976	-0.617	0.982
0.5x PBS	0.4402	-0.656	0.994
1.5x PBS	0.4641	-0.580	0.983
8.5 pH	0.4568	-0.606	0.988
10.0 pH	0.4410	-0.524	0.987

Graph 1: Viscosity of liquid porcine myocardial matrix at 25 C under standard conditions at 6 mg/ml and 8 mg/ml

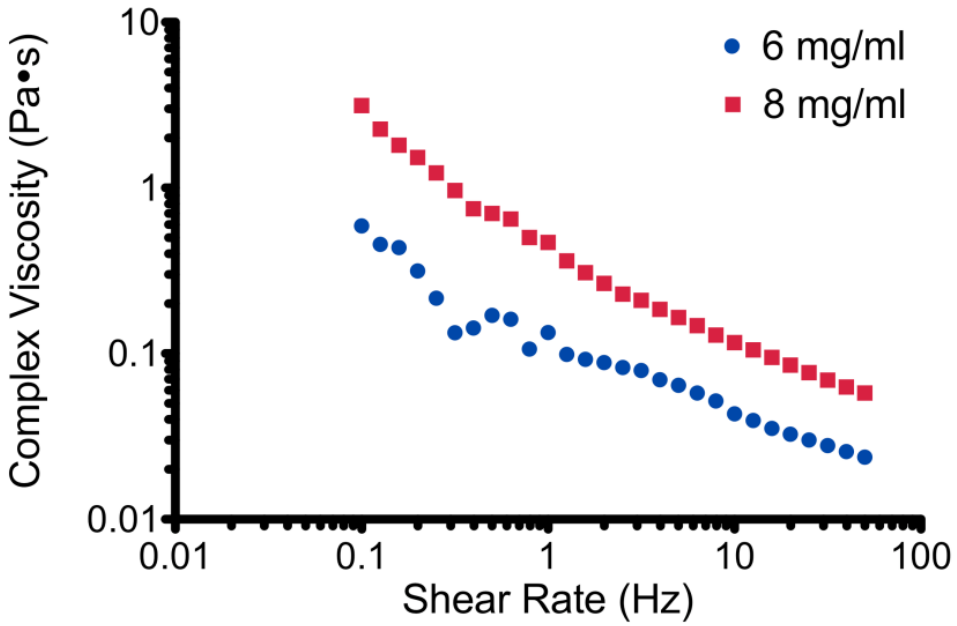

Table 4. Complex viscosity of the human myocardial matrix material at 25°C

Condition	*k*	*n*	r^2
Standard	0.1341	-0.572	0.920
IPA	0.2097	-0.555	0.955

Graph 2: Viscosity of human myocardial matrix compared to porcine myocardial matrix at 6mg/ml under standard conditions

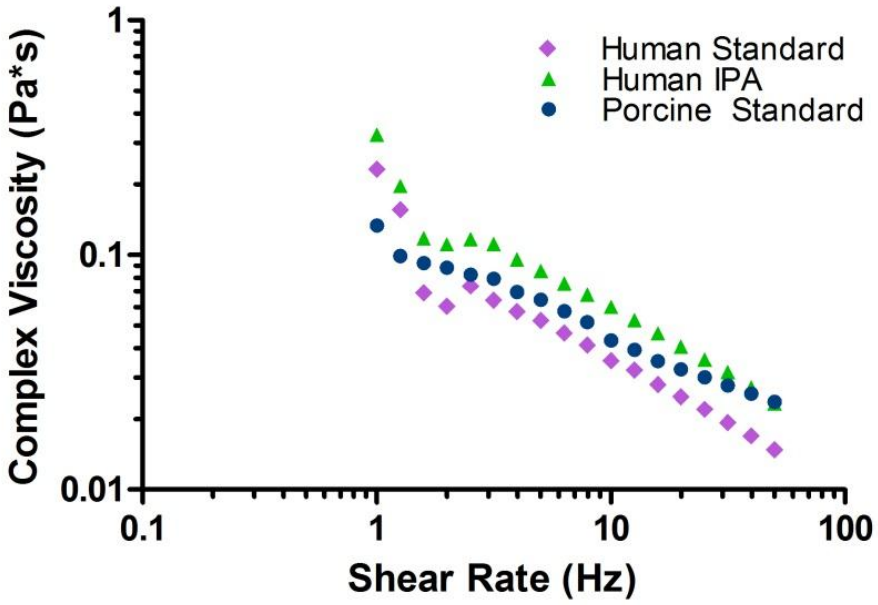

2.3.4 Swelling Ratio

The swelling ratios by mass for the five conditions at both material concentrations for the porcine myocardial matrix are summarized in table 5. The swelling ratios for the two different processing methods of the human myocardial

matrix are included in Table 6. There were no statistically significant variations between any of the groups.

Table 5 Swelling ratio of porcine ECM gels by mass after gelation at 37°C

Condition	6 mg/ml	8 mg/ml
Standard	58.42 ± 10.20	57.40 ± 2.39
0.5x PBS	55.90 ± 8.36	57.00 ± 1.19
1.5x PBS	56.42 ± 5.48	55.75 ± 4.68
8.5 pH	55.69 ± 4.34	56.18 ± 2.63
10.0 pH	59.84 ± 5.44	57.74 ± 5.59

Mean ± SD

Table 6. Swelling ratio of human ECM gels by mass after gelation at 37°C

Condition	6 mg/ml
Standard	65.84 ± 6.53
IPA	78.97 ± 11.15

Mean ± SD

2.3.5 Turbidimetric Gelation Kinetics

Marked changes in gelation kinetics were observed when varying salt concentration in the porcine myocardial matrix. As a result, a turbidimetric assessment was performed to quantify gelation kinetics. The absorbance of the gels at 405 nm wavelength was measured to analyze the turbidmetric gelation kinetics. The results for the material at 6 mg ml−1, as absorbance and normalized absorbance plotted over time, are shown in graph 3. The calculated parameters $t1/2$, t_{lag}, and S from the linear fits are summarized in table 7. The results for 1.5× PBS were omitted because of the long

gelation time. After 8 hour, the 1.5× PBS samples did not show an increase in absorbance and when visually inspected had not formed gels. When these gels were further incubated at 37 ◦C for a total of 16 h, gels were formed. Therefore, gelation time for 1.5× PBS samples ranged from 8 to 24 h. Changing the salt concentration had a significant effect on gelation kinetics. Samples with salt concentrations of 0.5× PBS had a significant decrease of $t1/2$ and increase of slope (table 7). This indicates that lowering salt concentration shortens the gelation time with an increase in the rate of gelation. Thus, the observations of dramatically slower gelation at 1.5× PBS were consistent with these findings.

The gelation kinetics for the human myocardial matrix was also quantified using turbidemetric assessment. The normalized absorbance plotted over time in graph 4 and the calculated parameters from the linear plot are summarized in table 8. The additional IPA step in the processing of the human myocardial matrix does not significantly affect gelation kinetics parameters when compared to the standard mode of processing. However, the human myocardial matrix gels gel considerably faster when compared to the porcine myocardial matrix at standard conditions, with a steeper slope, shorter T_{lag} and shorter $T_{1/2}$.

Graph 3: Turbidimetric Gelation Kinetics of Porcine Myocardial Matrix with varied salt concentration

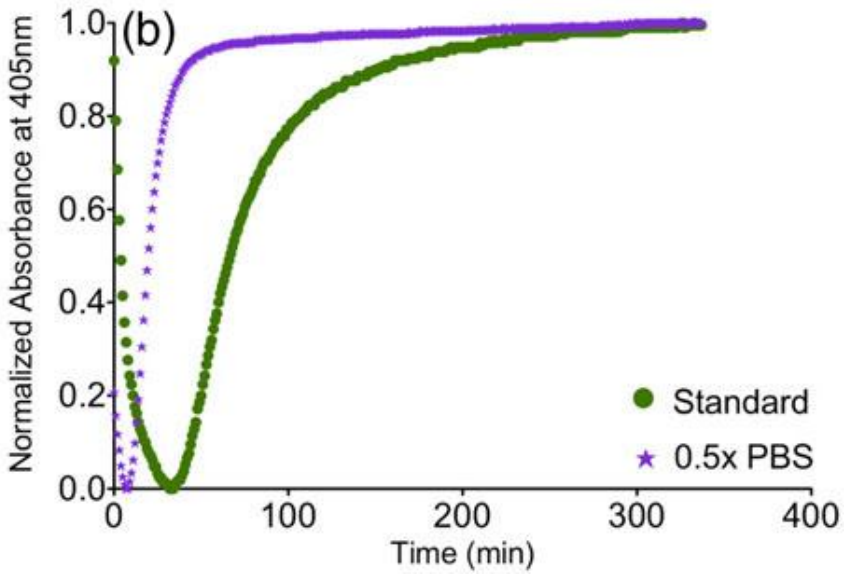

Table 7. Turbidity results for lag time (tlag) slope of linear region(S), and half gelation time (t1/2) of porcine myocardial matrix at 6mg/mL

Condition	t_{lag} (min)	S	$t_{1/2}$ (min)
Standard	40.28 ± 1.91	0.01867 ± 0.0012	67.14 ± 3.40
0.5x PBS	11.40 ± 2.17	0.05067 ± 0.0021	21.27 ± 2.33

Mean ± SD

Graph 4: Turbidimetric Gelation Kinetics of human myocardial matrix compared to porcine myocardial matrix

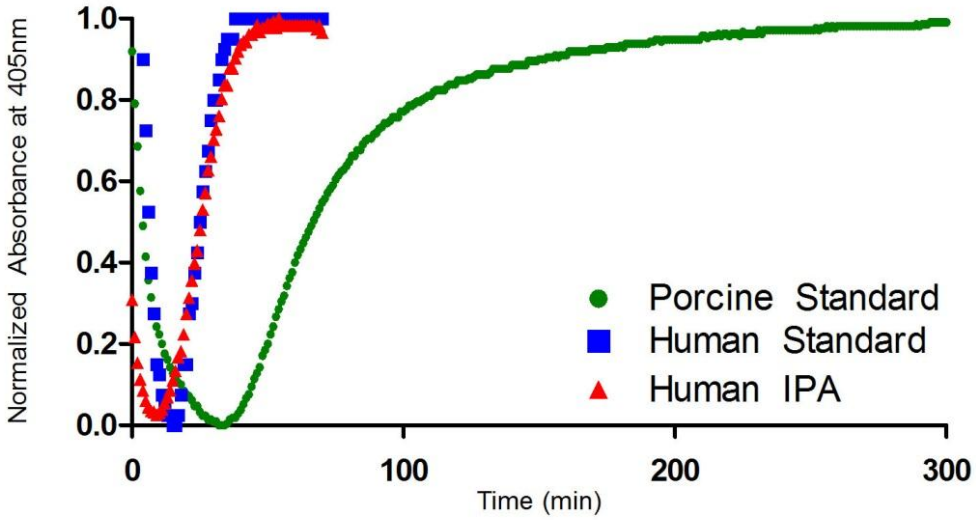

Table 8. Turbidity results for lag time (t_{lag}) slope of linear region(S) and half gelation time ($t_{1/2}$) of human myocardial matrix at 6mg/mL

Condition	t_{lag} (min)	S	$t_{1/2}$ (min)
Standard	19.57± 3.62*	0.0663 ± 0.0056	27.15 ± 4.24
IPA	14.25 ± 3.10	0.0471 ± 0.0037	24.91 ± 2.86

Mean ± SD

2.4 Discussion

In this study, an extracellular matrix hydrogel derived from porcine myocardial tissue was further characterized to increase the understanding of modulating its material properties. Particular interest was placed on the parameters of gelation including temperature, salt concentration, pH, and material concentrations because each has been previously shown to alter material properties of collagen hydrogels.

Salt concentration had the most dramatic impact on gelation kinetics. As salt concentration was increased, the rate of gelation decreased and the half time of gelation significantly increased. Under standard conditions, 6 mg/mL ECM hydrogels had a $t_{1/2}$ of 67.14 ±3.40 minutes upon incubation at 37 C. Decreasing the salt concentration to 0.5x PBS rapidly decreased the $t_{1/2}$ value to 21.27 ± 2.33 min. When the salt concentration was brought up to 1.5x PBS, there was no observed increase in turbidity in the first 8 hours, but a final gel was formed after 24 hours. Therefore it was confirmed that gelation time was between 8 and 24 hours, significantly greater than 67.14 ±3.40 minutes under standard conditions. The observation of increased gelation time with the increased amount of salt is consistent with results seen in collagen gels.

For the liquid form of the porcine myocardial matrix at 25 C, it was shown that with an increase in shear rate, a decrease in complex viscosity was observed. This phenomenon is known as shear thinning, which also occurs with collagen in the liquid form. The complex viscosity of the porcine myocardial matrix only differed with material concentration and did not differ for changes in pH or salt concentration. Viscosity is defined as the resistance of flow by a fluid and is affected by the degree of intramolecular and intermolecular forces. Therefore, the increase of complex viscosity at higher material concentrations can be explained by an increase of intermolecular force [59].

The swelling ratio of the material did not alter significantly when changing pH, salt concentration, or material concentration. This is not expected, since there were significant differences in the storage modulus between groups. The mass of the material

increased over 55 times its original dry weight when transitioning from a dry powder to a hydrogel. However, it should be noted that the standard deviations for the swelling ratios had a range of 2-20% of the mean value. Thus the variation between groups might have been masked by the large discrepancies within any groups.

When comparing the storage modulus of the porcine myocardial matrix to the two different human myocardial matrices, there was a significant difference between porcine and human myocardial matrix processed with standard protocol. However, when the human myocardial matrix was processed with IPA, the stiffness of the gel was the same as the porcine myocardial matrix (data for porcine myocardial matrix courtesy of Todd D. Johnson[58]). This observation may be explained by the lipid content of the myocardial matrix processed under standard protocol. Lipids, having both a hydrophilic and hydrophobic region, may have altered hydrophilic interactions in collagen proteins during self-assembly and thus yielding a significantly weaker gel[60].

The complex viscosities of the liquid human myocardial matrix were comparable to the viscosities of the liquid porcine myocardial matrix. However, a slight increase in viscosity was observed when the human tissue was treated with IPA during the decellularization process when compared to the standard processing. IPA solubilizes lipids as well as certain glycosaminoglycans but leaves proteins intact. The slight increase of viscosity may be explained by an overall increase in protein concentration in the end processing of the human myocardial matrix. The swelling ratios of the human myocardial matrix did not significantly differ from the each other and from the porcine myocardial matrix.

The gelation kinetics of the human myocardial matrix did not significantly differ based on the mode of processing. However, the human myocardial matrix gelled significantly faster than the porcine myocardial matrix at the same standard conditions. The standard human myocardial matrix had a $t_{1/2}$ of 27.15 ± 4.24 minutes. These differences may be attributed to the inherent differences in biochemical composition of the extracellular matrices between species, however further biochemical analysis will be required to determine what differences exist.

2.5 Conclusion

When selecting a biomaterial for injectable delivery, the material properties are very important parameter to understand. Collagen is a commonly used biomaterial and many of its properties have been characterized. In addition, tailoring the mechanical properties by varying gelation parameters has also been explored previously. However, no studies have been conducted to characterize the material properties of the decellularized ECM hydrogels. Therefore, this study aimed to better characterize mechanical properties of the naturally derived ECM hydrogel and demonstrated that the mechanical properties can be modulated by changing gelation conditions.

From this study, it was established that the ECM material readily gels when brought to 37 C. At 37 C, the rate of gelation can be controlled and increased from about 20 minutes to over 8 hours by increasing the salt concentration. In addition, changing the salt concentration also showed a decrease in the storage modulus of the material. It was also demonstrated that the increase in material concentration led to an increased viscosity in its liquid form. Overall, this study demonstrated that some

material properties of the ECM material and those properties can be tailored. This can be useful for the future development of the material for *in vitro* and *in vivo* when optimum properties for the material are determined.

CHAPTER THREE:

CELLULAR BEHAVIOR ON A CARDIAC EXTRACELLULAR MATRIX HYDROGEL

3.1 Introduction

Cell culture of mammalian cells has served as a platform to investigate cell and tissue physiology and pathophysiology outside of an organism. The traditional approach is to culture cells on two-dimensional substrates like polystyrene tissue culture plates. For years, the cells cultured in these 2D settings have provided a base for observing complex processes, such as stem cell differentiation, proliferation, and gene expression.

However, recent work has shown that cells will often exhibit unnatural behavior when cultured on 2D polystyrene constructs and confined to a cell monolayer[61]. In an early study, stark differences were observed between human breast epithelial cells grown on a 2D monolayer compared to 3D analogs[62]. In 2D, the cells developed tumor cells, but when grown in 3D, they assumed normal growth behavior. Furthermore, work by Engler et al demonstrated that the differentiation of human mesenchymal stem cells is dependent on the mechanical stiffness of the 2D culture platform [63]. These results show the limitations of traditional cell culture on polystyrene tissue culture surfaces.

Recently, there has been recent interest in designing three-dimensional scaffolds that mimic the native cellular environment for in vitro cell culture. Extracellular matrix hydrogels such as collagen, fibrin, hyaluronic acid and Matrigel have been explored as scaffolds to observe cellular response in vitro[61]. These materials are derived from natural sources and are inherently biocompatible. They have been shown to promote cellular function, proliferation, and viability. However, with the exception of Matrigel, these ECM materials are of single components and do not fully mimic the complex

native cellular environment. Matrigel is a complex mixture of ECM components, but it is derived from a mouse sarcoma cell line and cannot accurately represent native tissue composition.

With the development of decellularization technology, extracellular matrix hydrogels that mimic the native tissue's complex composition can be made. The myocardial matrix is one example. In recent work by DeQuach et al[46], when human embryonic stem cell derived cardiomyocytes were plated on myocardial matrix coated tissue culture surfaces, increased rates of maturation were observed when compared to standard gelatin coatings. This demonstrates the advantageous changes in cellular behavior by the myocardial extracellular matrix.

Because the myocardial matrix has been shown to be advantageous as a coating, this study aims to determine the feasibility of using the myocardial matrix in a hydrogel form as a platform to study cellular phenomenon *in vitro*. The cytocompatibility of the hydrogel was first assessed using a live/dead stain, the cell attachment was assessed using a MTT dye reagent, and cell proliferation was assessed using Picogreen dsDNA reagent and MTT dye reagent. Finally, cellular infiltration was assessed by cryosectioning and staining with Hematoxylin and Eosin.

3.2 Materials and Methods

3.2.1 Hydrogel Formation

The myocardial ECM and rat-tail collagen type I hydrogels were formed using methods stated in section 2.2.X. In short, the pH and salt concentration of the enzymatically digested cardiac ECM and rat-tail collagen type I were adjusted to physiological conditions (pH 7.4 and 1x PBS) using 1.0M NaOH and 10X PBS respectively on ice. The concentration of each was adjusted with 1x PBS end concentration of 6.0mg/mL for the cardiac ECM and 2.5mg/mL for the rat-tail collagen allowed to fully gel at 37C. For the subsequent cell viability, cell attachment, MTT assay, and Picogreen assay, 50µL ECM or collagen gels were formed in 96 well plates. For the invasion study, 500µL ECM gels were formed using a 4mL scintillation vial.

3.2.2 Matching Rheological Properties

Rheological measurements of both ECM and collagen I hydrogels were made with a TA Instruments ARG2 Rheometer, following the protocol stated in section 3.2.1. In brief, 500uL collagen type I gels were made ranging from 2mg/mL to 5mg/mL and ECM gels were made at 6mg/ml. The storage modulus (*G*') over frequencies of 0.04–16 Hz was recorded and the storage modulus at 1 rad s−1 or 0.16 Hz was compared.

3.2.3 Cell culture

Rat aortic smooth muscle cells RASMCs were chosen for the study because it was previously shown that these cells migrate into the ECM and contribute to

neovascularization in vivo[10]. Therefore, we wanted to investigate the behavior of these cells in vitro. RASMCs were isolated from 3 month old Harlan Sprague–Dawley rats, as previously described[10]. In short, the aorta was isolated, free adventitia was removed, and endothelial cells were rinsed off. Following, the aorta was minced into small pieces and RASMCs were grown out of explants. The cells were cultured in growth media , containing phenol-red free DMEM supplemented with 10% Fetal Bovine Serum (FBS) and 1% penicillin/streptomycin and split 1:4 using trypsin when 80% confluent. Phenol-red was excluded from the media because it has been shown to interfere with many biochemical assays. Cells passages 4-9 were used for experiments.

3.2.4 Cell Viability

RASMCs were seeded on the top surface of the gels in 96-well plates at a density or 20,000cells/well with media changes every 2 days. The cell viability of the RASMCs grown on the ECM hydrogels were assessed at 24 hours, 3 days, 5 days, 7 days and 10 days after initial seeding using a live/dead assay (Invitrogen, Carlsbad, CA) following manufacturer's protocol. At the given time points, the ECM hydrogels were washed with PBS and incubated in a solution of 1.0 μL of Calcein AM and 1 μL of ethidium homodimer-1 in 1 mL PBS (calculate out concentrations later) for 30 minutes. The gels were then rinsed 2x with PBS and imaged using a Zeiss Axiovision microscope.

3.2.5 Cell Attachment

Cell attachment of the RASMCS onto the hydrogels was assessed using a modified version of a previously published protocol [64]. Porcine ECM and collagen type I hydrogels were prepared as described in section 3.2.1. RASMCs were seeded on the top surface of the porcine ECM hydrogel, collagen I hydrogel, or uncoated polystyrene at a density of 50,000 cells per well in a 96-well plate. Wells with each type of gel incubated with media but without cells served as controls. At different time points, 15 minutes, 30 minutes, 45 minutes, 1 hour, 1.5 hours, the wells were rinsed with PBS three times to remove any non-adherent cells. 100 uL of fresh growth media supplemented with 0.33mg/mL MTT reagent was added to each well and incubated for 4 hours. During this time, the pale yellow MTT reagent is being cleaved by living cells, yielding a purple formazan product. After incubation, MTT reagent and media were carefully removed. 200uL of DMSO were then added to each well and the plate was put on a shaker for 5 minutes to fully dissolve the purple formazan crystals. The plate was read for absorbance at 570nm wavelength using a Synergy™ 4 Multi-Mode Microplate Reader (Biotek).

3.2.6 MTT Assay

RASMC were seeded on the surface of the myocardial ECM or collagen hydrogels at a density of 20,000 cells per well and media was changed every other day. Gels with media but without cells served as controls. The relative metabolic activity of the cells in each condition was quantified at 24 hours, 3 days, 5 days and 7 days using

the MTT assay. At the given time points, the cells were briefly washed with PBS to remove non-adherent cells. The cells were incubated in growth media supplemented with 0.33mg/mL MTT reagent for 4 hours. During this time, the pale yellow MTT reagent is being cleaved by living cells, yielding a purple formazan product. After incubation, MTT reagent and media were carefully removed. 200µL of DMSO were then added to each well and the plate was put on a shaker for 5 minutes to fully dissolve the purple formazan crystals. The plate was read for absorbance at 570nm wavelength using a Synergy™ 4 Multi-Mode Microplate Reader (Biotek).

3.2.7 Picogreen Assay

RASMC were seeded on the surface of the ECM or collagen hydrogels at a density of 20,000 cells per well and media was changed every other day. Gels with media but without cells served as controls. To assess overall cell proliferation on the hydrogels, the total DNA content was quantified using the Quant-iT Picogreen kit (Invitrogen, Carlsbad, CA) at 24 hours, 3 days, 5 days and 7 days. Media was aspirated from the wells and the hydrogels were washed with PBS to remove non-adherent cells. Each sample was then frozen at -80C and thawed at room temperature to lyse the cells. The hydrogel scaffolds were then digested with 100µL of 0.5mg/mL Proteinase K(Invitrogen, Carlsbad, CA) at 60C overnight. Total hydrogel digestion was confirmed by observing a clear homogeneous liquid in each well. The samples were then transferred to a 96-well plate and 100uL of Picogreen reagent was added to each

sample. A standard was prepared using λ bacteriophage DNA. The plates were read at 485/538 nm using a Synergy™ 4 Multi-Mode Microplate Reader (Biotek).

3.2.8 Cellular Infiltration

The growth and invasion of the RASMCs in the ECM hydrogels were evaluated by histological methods. Disks of ECM hydrogel were made by using a 4mL scintillation vial as a mold. After the ECM hydrogel was completely gelled, it was incubated in growth medium for 24 hours. RASMS were seeded on the top surface of the gel at density of 50,000 cells per gel. The medium was changed every other day until the cells reached visible confluence under light microscopy at 7 days. The samples were then frozen in Tissue Tek O.C.T. freezing medium, sectioned at 20um slices, and stained using Hematoxylin and Eosin (H&E).

3.2.9 Scanning Electron Microscopy

ECM gels were cross-linked with 2.5% glutaraldehyde (Sigma-Aldrich, Grade II, 25%, St Louis, MO) for 2 h then dehydrated with a series of ethanol washes of increasing concentration (30%, 50%, 75%, and 100%). The gels were critical point dried from ethanol in CO2 using a Tousimis AutoSamdri 815A. Samples were mounted and then sputter coated with chromium (Cr) or iridium (Ir) using an Emitech K575X Sputter Coater. Imaging was done with a FEI XL30 UHR SEM.

3.3 Results

3.3.1 Matching Rheological Properties

To determine an appropriate control for the subsequent cell studies, the storage modulus (G') of the 6mg mL ECM hydrogels were matched to a collagen type I hydrogel. Matching the rheological properties was done because previous studies have shown mechanical stiffness of a hydrogel affects multiple aspects of cellular behavior, including attachment, proliferation, and metabolic activity. A collagen hydrogel of 2.5mg mL was found to have a storage modulus that was not significantly different than the 6 mg mL ECM hydrogel and was chosen as a control for subsequent studies (data not shown).

3.3.2 Cell Viability

Initial cell viability of the cells cultured on the ECM hydrogel was first assessed using a live/dead stain. The calcein AM is actively transported through the cellular membrane of living cells and becomes trapped. It is then converted by esterase in the cell into a green fluorescent calcein, which has an excitation and emissions of wavelengths 495/515nm respectively. In contrast, the ethidium homodimer-1 is a cell-impermeant indicator that has a high-affinity nucleic acid. In dead cells, the cell membrane becomes compromised, allowing the ethidium homodimer-1 to bind to the DNA in the cell nucleus. Thus, the green fluorescence indicates cell viability and the red fluorescence indicates dead cells. After 24 hours after initial seeding, the RASMCs

cultured on the cardiac ECM hydrogel attach and the majority of the cells are viable. Over the course of the ten day culture, the cell viability remains relatively the same and the cells are seen to proliferate. By day 10, the cells form dense confluent sheets as seen in Figure 2e.

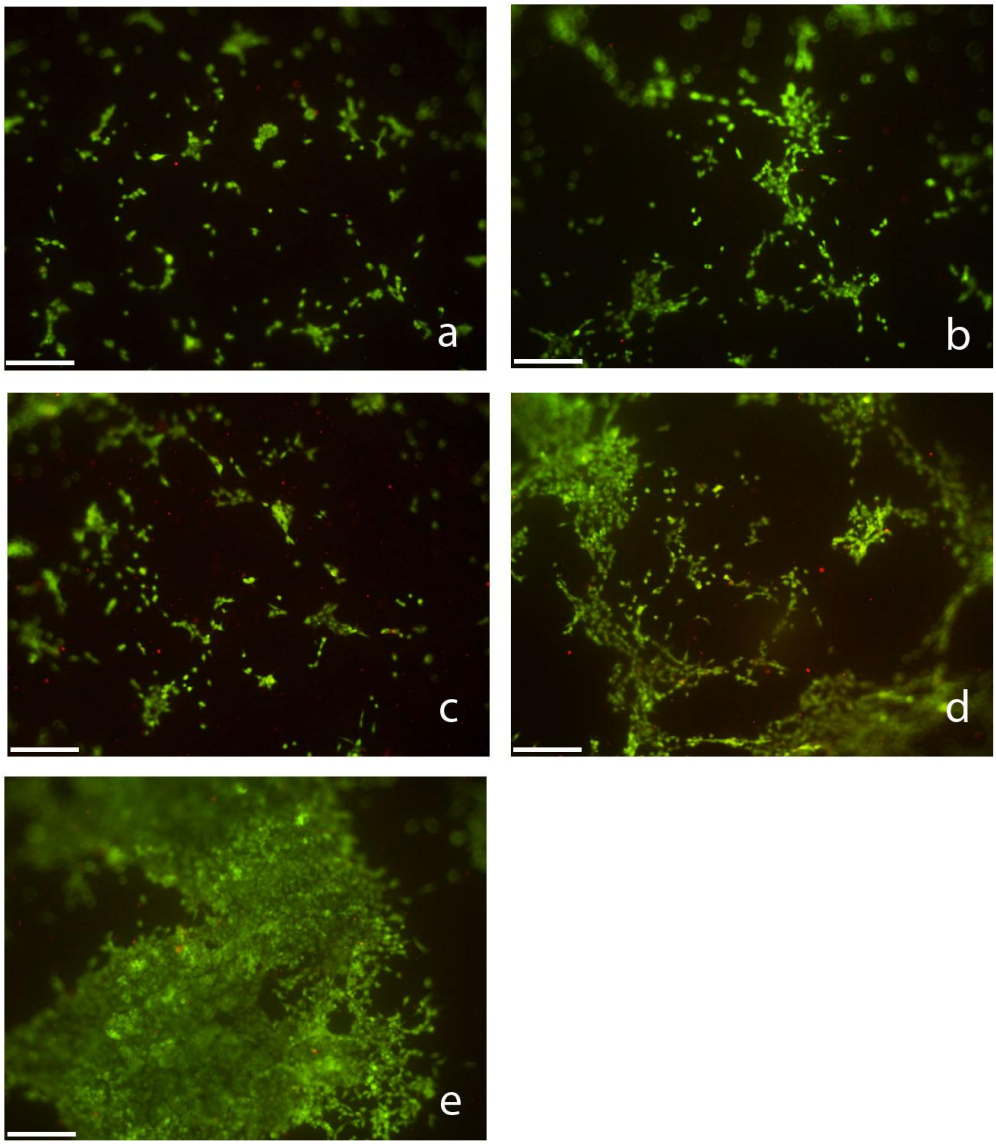

Figure 2: RASMC cell viability over span of ten days. (a) day 1, (b) day 3, (c) day 5, (d) day 7, (e) day 10; Scale bar = 200µm

3.3.3 Cell Attachment

Using the MTT dye reagent, the rate of cell attachment on the ECM gel, collagen gel, and uncoated polystyrene surfaces were assessed. The MTT is quickly metabolized by the mitochondria in the cells through the enzyme succinate dehydrogenase to yield purple formazan crystal. The crystals can be dissolved and the absorbance read to give a quick, simple, and sensitive way to determine the overall quantity of live cells attached to a substrate in a microwell plate. Graph 5 shows the attachment of RASMCs when seeded on uncoated polystyrene, collagen gels, and ECM gels over a time period of 180 minutes. The results show that the polystyrene supports the most cell adhesion, followed by collagen gels and then ECM gels.

Graph 5: Attachment of RASMC over time

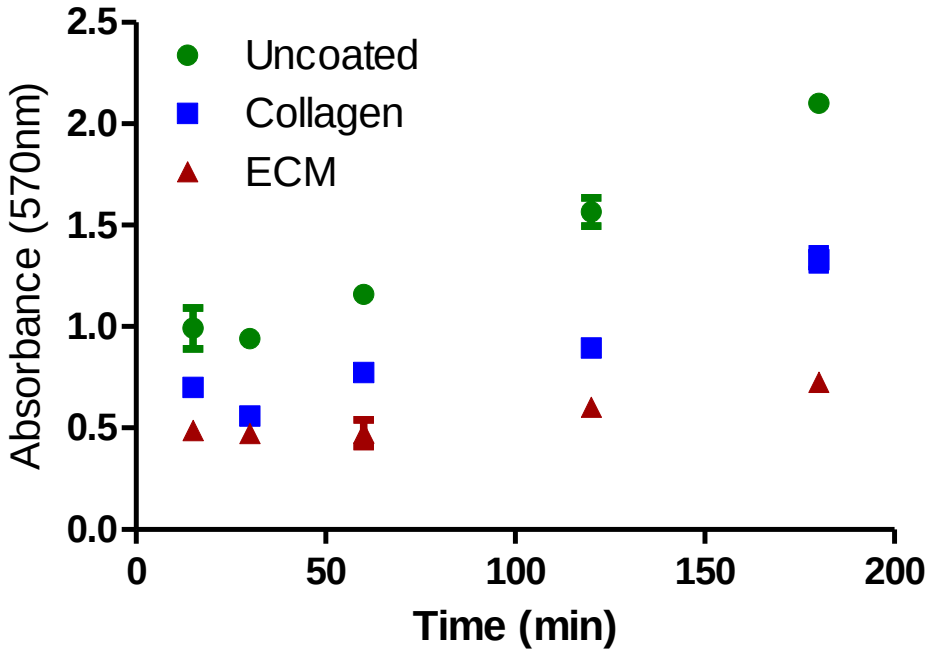

3.3.4 MTT Assay

The MTT dye reagent was also used to assess the proliferative properties of the RASMCs cultured on uncoated polystyrene, collagen gels, and ECM gels. Graph 6 shows the comparison in cell number over the course of 7 days. Data from cells cultured on polystyrene were excluded from the plot because the cell number exceeded the range of the assay by day 3, indicating a much higher rate of proliferation when compared to the collagen and ECM gel conditions. At each time point, there were significantly more cells on the collagen gels when compared to the ECM gels. ($p < 0.01$)

Graph 6: MTT of RASMC over 7 days on ECM and Collagen gels

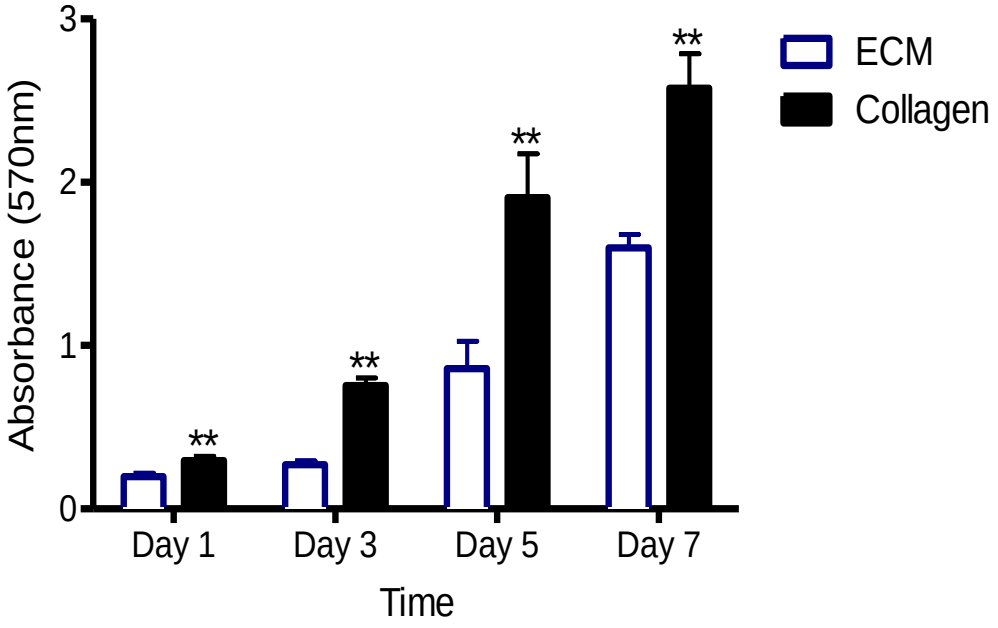

3.3.5 Picogreen Assay

To confirm the results observed in the previous MTT assay, a picogreen assay was performed to assess total DNA content present on the uncoated polystyrene, collagen gel, and ECM gel. The picogreen reagent is a fluorescent nucleic acid stain for double stranded DNA in solution. The picogreen reagent does not fluoresce, but upon binding to dsDNA, it exhibits a > 1000-fold fluorescence enhancement. Thus the fluorescence intensity of a sample can be related to the overall DNA content of a sample. Graph 7 shows the comparison in total DNA content of the cells grown on collagen and ECM gels over the span of 7 days. Data from cells cultured on polystyrene were excluded from the plot because the cell number exceeded the range of the assay by day 5, indicating a much higher rate of proliferation when compared to the collagen and ECM gel condition. For days 1 and 3, there is significantly more DNA content ($p < 0.01$) for collagen gels as compared to ECM gels, which represents more cells being present on collagen gels. On day 5, the significance drops ($p<0.05$) and on day 7 the significance between the two conditions disappears. However, there is a clear trend showing that there are more cells present on collagen gels when compared to ECM gels.

Graph 7: Picogreen DNA Quantification

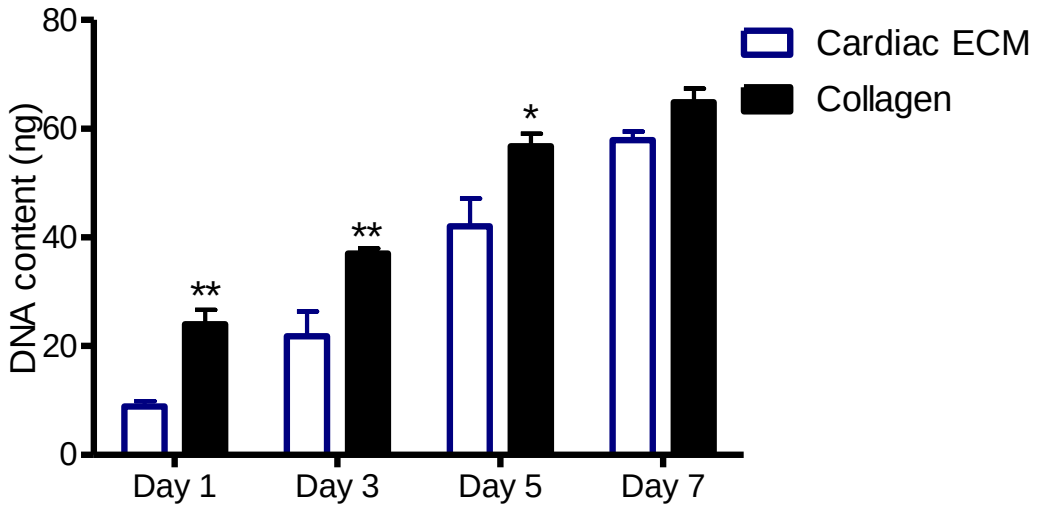

3.3.6 Cellular Infiltration

The RASMCs cultured on top of the ECM hydrogels were able to grow and proliferate. After 7 days in culture, the cells formed a multilayer of cells on top of the gel as seen in Fig 3. The cells did not migrate through the gel and remained on the top surface of the gel.

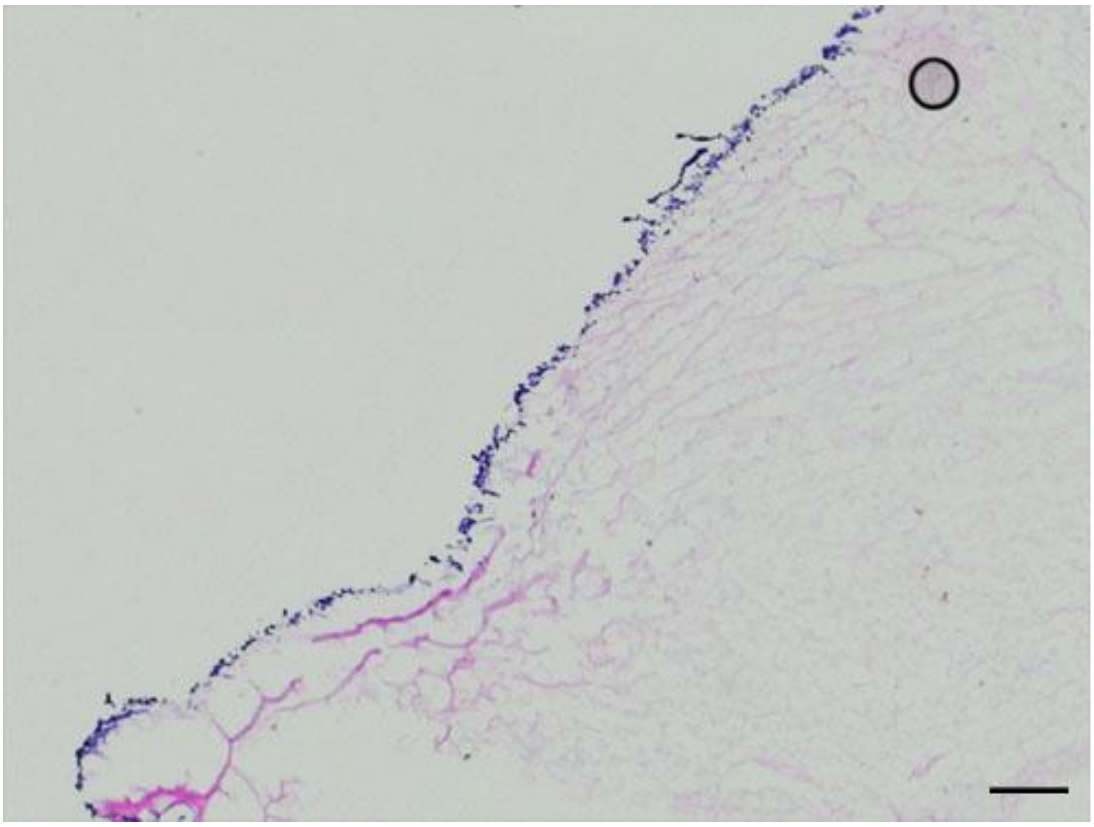

Figure 3: RASMC multilayer after 7 days. Scale bar = 100µm

3.3.7 Scanning Electron Microscopy

To assess the limited cellular migration observed with RASMCs are cultured on ECM hydrogels, SEM images were taken. The ECM hydrogels were previously shown to be a nanofibrous, mesoporous in structure. It was expected that cells would migrate through the porous network of ECM hydrogel. However, the surface of the hydrogel forms a smooth, continuous shell as seen in figure 4a. The thin shell surrounds the nanofibrous structure which can be observed in a cross sectional image in figure 4b. The presence of a continuous shell may explain why limited migration is observed.

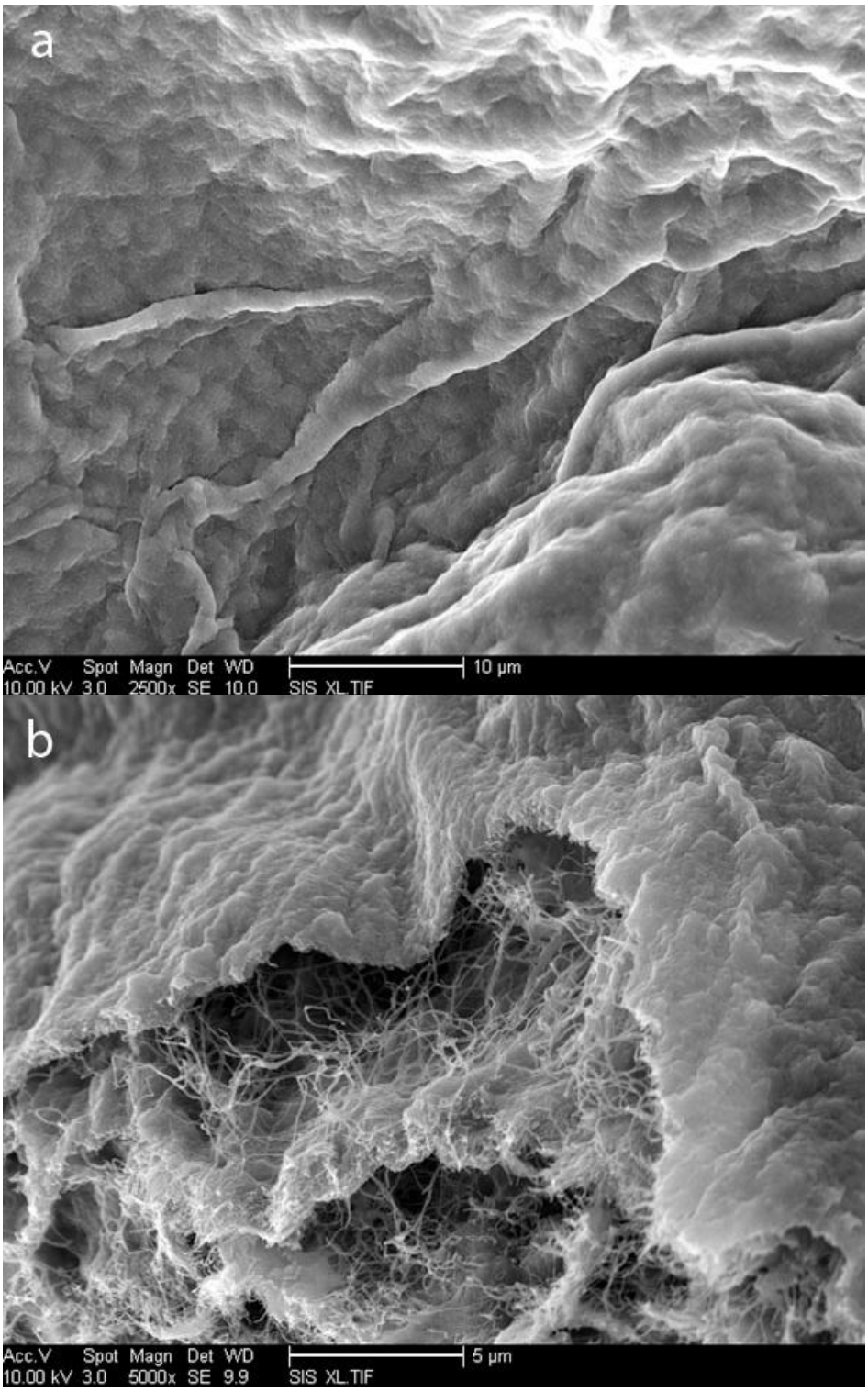

Figure 4: SEM images showing the (a) surface of the ECM hydrogel and (b) the cross sectional view of the ECM hydrogel with the nanofibrous center

3.4 Discussion

In this study, the porcine myocardial matrix was characterized for its *in vitro* cytocompatibility. Rat aortic smooth muscle cells (RASMCs) were chosen for this study because they have been previously shown to be involved in neovascularization *in vivo.* To assess initial cytocompatibility, the cells were seeded on the top surface of the ECM hydrogels and observed for both survival and growth using a live/dead stain. The results show that the vast majority of the cells survive on the ECM gel and continue to proliferate to form dense monolayers, thus confirming the cytocompatibility of the ECM material.

After confirmation of biocompatibility, cellular behavior on the surface of the myocardial matrix hydrogel was compared to a collagen I hydrogel, which is a commonly used hydrogel for tissue culture applications. To eliminate the effects of different gel stiffness, the concentration of the collagen I gels was adjusted to match the rheological properties of the cardiac ECM gels. When comparing the attachment of the RASMCs on uncoated polystyrene, collagen gels and ECM gels, the cells significantly adhered more to the polystyrene surfaces. This is expected, since several studies have indicated that cells will preferentially attach to stiffer surfaces. However, when comparing the RASMC attachment on collagen I gels with the ECM gels, there was significantly more attachment on the collagen I gels. This result is not surprising because the ECM gels have a different composition that includes proteoglycans and glycosaminoglycans that may interfere with cell adhesion[65]. Proteoglycans in the ECM can interact with cell adhesion ECM ligands and interfere with cell adhesion.

Small interstitial dermatan sulfate and decorin are some examples of proteoglycans that interfere with cellular adhesion [66].

When comparing the proliferative abilities of the RASMCs on the three different surfaces, the polystyrene showed the highest levels of cell proliferation. The cell number got so high and exceeded the range of both assays. When cells are seeded on extremely stiff 2D surfaces such as polystyrene, they assume a synthetic phenotype and are extremely proliferative. The decreased in proliferative abilities on the ECM hydrogels when compared to collagen I gels may be also explained by the rich proteoglycan and glycosaminoglycan content. The anti-proliferative properties of heparin and heparin sulfate RASMCs have been well documented [67-72]. In addition, over-sulfated glycosaminoglycans, such as chondroitin and dermatan sulfate have been shown to further decreases cell proliferation [73].

The invasive properties of RASMCs were explored using H&E analysis. Previously, in vivo, RASMCs and endothelial cells were shown to infiltrate the gel and form arterioles. However, *in vitro*, very little migration into the gel was observed. Instead, the cells formed confluent multilayer of cells on the top surface of the gel. Upon further inspection using SEM, the ECM hydrogels are shown to form a shell around the porous nanofibrous structure previously described, which may have inhibited the cell's ability to migrate through. In addition, the continuous shell may have also prevented nutrients from the media to freely diffuse into the center of the gel, creating a less ideal environment for cells. As a result, the cells remain in the nutrient rich outer region and are not attracted to the nutrient void interior.

3.5 Conclusion

This study demonstrated that cells readily adhere to the ECM hydrogel *in vitro.* Once adhered, the cells proliferate to form a monolayer on the top surface of the hydrogel. These results suggest that the ECM hydrogel can be used as a potential platform to study cellular behavior *in vitro.*

CHAPTER FOUR:

CONCLUSION AND FUTURE DIRECTIONS

4.1 Conclusion

Heart failure continues to be one of the leading causes of death in the western world and it is evident that alternative treatments need to be developed. Recent strategies have taken tissue engineering approaches to develop biological scaffolds to facilitate the repair of damaged heart tissue. In particular, ECMs that are derived from decellularizing native tissue have been explored by a number of groups for cardiac tissue engineering. Decellularized materials are promising because they take advantage of nature's platform to create an intrinsically complex extracellular matrix scaffold that is thought to mimic the native extracellular matrix environment. The myocardial matrix, being derived from the myocardium, is thought to contain cardiac specific cues for cell-matrix interactions in the heart, making it a suitable scaffold for cardiac tissue engineering. The myocardial matrix can be processed into an injectable form that will self-assemble into a hydrogel under physiological conditions.

To better understand the myocardial matrix material, material properties including viscosity, swelling ratio, and gelation kinetics of the porcine myocardial matrix were determined. When gelation conditions of pH, salt concentration, or protein concentration were altered, there were significant changes in some of the material properties. Higher salt concentration was shown to significantly slow the rate of gelation. Higher protein concentration was shown to increase viscosity due to the increase in intermolecular forces. There was no significant change in swelling ratio observed when gelation conditions were changed.

Differences between human and porcine myocardial matrix were observed in stiffness and in gelation kinetics. The human myocardial matrix was less stiff and gelled at a faster rate when compared to the porcine myocardial matrix. There was no significant difference between the observed swelling ratios.

The porcine myocardial matrix was shown to support smooth muscle cell attachment and growth *in vitro* under static conditions. When compared to a collagen I gel of the same stiffness, there was significantly more attachment and proliferation on the collagen I gels. When the smooth muscle cells were cultured on the myocardial matrix gel, the cells formed a confluent multilayer of cells on the surface and did not migrate through the material. On inspection of the SEM images, a phase separation occurs and a shell is formed around the porous nanofibrous center. This shell may be hindering the diffusion of nutrients to the center of the hydrogel. With a nutrient deficiency in the center, the cells remain on the top surface of the hydrogel and do not migrate into the hydrogel.

Overall, this work further characterizes the myocardial matrix hydrogel and contributes to our understanding of the behavior of this material. The results demonstrate that some mechanical properties, such as storage modulus and gelation kinetics, can be modulated by changing gelation conditions. This study also validates the feasibility of the myocardial hydrogel to be used as a platform to study cell hydrogel interactions *in vitro*. Both results greatly increase our understanding of the myocardial matrix material and will aid in the future development of the material as a potential treatment for MI.

4.2 Future Directions

The major limitation in this study is the fact that the myocardial matrix is a naturally derived material, which suffers from batch-to-batch variability. Therefore, it may be difficult to repeat the results when different batches of extracellular matrix are used for experimentation.

There were observable differences between the human myocardial matrix and the porcine myocardial matrix. However, currently, there are too many variables present to determine the reason behind the differences in material properties. Further biochemical analysis may help answer these questions. Mass spectrometry can be used to help determine the different components of the human myocardial matrix. Collagen content in both materials can be determined through the use of western blots or the use of a Sircoll assay kit. Also, differences may have been due to age differences, since age has been shown to increase collagen content in the native cardiac extracellular matrix[74].

This study validated the *in vitro* cytocompatibilty of the myocardial matrix hydrogel. Further studies can now be done to assess cellular behavior when cultured on top of the ECM gel. For example, qPCR analysis, western blots, and immunostaining for alpha-smooth muscle actin (SMA) can determine differences in differentiation. Since no migration was observed with the RASMCs were cultured on top of the hydrogel, cellular behavior could be assessed when encapsulated in the extracellular matrix hydrogel. This will give the cells access to the nanofibrous interior and help question if the limited migration is actually due to the shell formation or a diffusion

limitation in nutrients. Studying cellular behavior in this 3D environment may also prove to be a better model for studying cell-matrix interactions.

REFERENCES

1. Roger VL, Go AS, Lloyd-Jones DM, Benjamin EJ, Berry JD, Borden WB, Bravata DM, Dai S, Ford ES, Fox CS, Fullerton HJ, Gillespie C, Hailpern SM, Heit JA, Howard VJ, Kissela BM, Kittner SJ, Lackland DT, Lichtman JH, Lisabeth LD, Makuc DM, Marcus GM, Marelli A, Matchar DB, Moy CS, Mozaffarian D, Mussolino ME, Nichol G, Paynter NP, Soliman EZ, Sorlie PD, Sotoodehnia N, Turan TN, Virani SS, Wong ND, Woo D, Turner MB (2012) Heart Disease and Stroke Statistics--2012 Update: A Report From the American Heart Association. Circulation 125: e2-e220.

2. Anversa P, Nadal-Ginard B (2002) Myocyte renewal and ventricular remodelling. Nature 415: 240-243.

3. Sun Y, Weber KT (2000) Infarct scar: a dynamic tissue. Cardiovasc Res 46: 250-256.

4. Pfeffer MA, Braunwald E (1990) Ventricular remodeling after myocardial infarction. Experimental observations and clinical implications. Circulation 81: 1161-1172.

5. Pfeffer JM, Pfeffer MA, Fletcher PJ, Braunwald E (1991) Progressive ventricular remodeling in rat with myocardial infarction. Am J Physiol 260: H1406-1414.

6. Bonvini RF, Hendiri T, Camenzind E (2005) Inflammatory response post-myocardial infarction and reperfusion: a new therapeutic target? European Heart Journal Supplements 7: I27-I36.

7. Jugdutt BI (2003) Ventricular remodeling after infarction and the extracellular collagen matrix: when is enough enough? Circulation 108: 1395-1403.

8. Holmes JW, Borg TK, Covell JW (2005) Structure and mechanics of healing myocardial infarcts. Annu Rev Biomed Eng 7: 223-253.

9. Anversa P, Beghi C, Kikkawa Y, Olivetti G (1986) Myocardial infarction in rats. Infarct size, myocyte hypertrophy, and capillary growth. Circ Res 58: 26-37.

10. Singelyn JM, DeQuach JA, Seif-Naraghi SB, Littlefield RB, Schup-Magoffin PJ, Christman KL (2009) Naturally derived myocardial matrix as an injectable scaffold for cardiac tissue engineering. Biomaterials 30: 5409-5416.

11. Wolfe RA, Roys EC, Merion RM (2010) Trends in organ donation and transplantation in the United States, 1999-2008. Am J Transplant 10: 961-972.

12. Welsh RC, Goldstein P, Adgey J, Verheugt F, Bestilny SA, Wallentin L, Van de Werf F, Armstrong PW (2004) Variations in pre-hospital fibrinolysis process of

care: insights from the Assessment of the Safety and Efficacy of a New Thrombolytic 3 Plus international acute myocardial infarction pre-hospital care survey. Eur J Emerg Med 11: 134-140.

13. Rickles FR (2005) Thrombolytic (fibrinolytic) drugs and progress in treating cardiovascular disease. FASEB J 19: 671.

14. Armstrong PW, Collen D, Antman E (2003) Fibrinolysis for acute myocardial infarction: the future is here and now. Circulation 107: 2533-2537.

15. Georgescu A, Fu Y, Yau C, Hassan Q, Luchansky J, Armstrong PW, Wagner G, Van de Werf F, Goodman SG (2005) Short- and long-term outcomes of patients with electrocardiographic left ventricular hypertrophy after fibrinolysis for acute myocardial infarction. Am J Cardiol 96: 1050-1052.

16. (1993) The Effects of Tissue Plasminogen Activator, Streptokinase, or Both on Coronary-Artery Patency, Ventricular Function, and Survival after Acute Myocardial Infarction. New England Journal of Medicine 329: 1615-1622.

17. Gottlieb SS, McCarter RJ, Vogel RA (1998) Effect of Beta-Blockade on Mortality among High-Risk and Low-Risk Patients after Myocardial Infarction. New England Journal of Medicine 339: 489-497.

18. Califf RM, Topol EJ, Stack RS, Ellis SG, George BS, Kereiakes DJ, Samaha JK, Worley SJ, Anderson JL, Harrelson-Woodlief L (1991) Evaluation of combination thrombolytic therapy and timing of cardiac catheterization in acute myocardial infarction. Results of thrombolysis and angioplasty in myocardial infarction--phase 5 randomized trial. TAMI Study Group. Circulation 83: 1543-1556.

19. Lonn E, McKelvie R (2000) Drug treatment in heart failure. BMJ 320: 1188-1192.

20. McCarthy PM, Schmitt SK, Vargo RL, Gordon S, Keys TF, Hobbs RE (1996) Implantable LVAD infections: Implications for permanent use of the device. Annals of Thoracic Surgery 61: 359-365.

21. Kinoshita M, Takano H, Taenaka Y, Mori H, Takaichi S, Noda H, Tatsumi E, Yagura A, Sekii H, Akutsu T (1988) Cardiac disuse atrophy during LVAD pumping. ASAIO Trans 34: 208-212.

22. Rane AA, Christman KL (2011) Biomaterials for the treatment of myocardial infarction a 5-year update. J Am Coll Cardiol 58: 2615-2629.

23. Blom AS, Pilla JJ, Arkles J, Dougherty L, Ryan LP, Gorman JH, Acker MA, Gorman RC (2007) Ventricular restraint prevents infarct expansion and improves borderzone function after myocardial infarction: A study using magnetic resonance imaging, three-dimensional surface modeling, and myocardial tagging. Annals of Thoracic Surgery 84: 2004-2010.

24. Fujimoto KL, Ma ZW, Nelson DM, Hashizume R, Guan JJ, Tobita K, Wagner WR (2009) Synthesis, characterization and therapeutic efficacy of a biodegradable, thermoresponsive hydrogel designed for application in chronic infarcted myocardium. Biomaterials 30: 4357-4368.

25. Wang T, Wu D-Q, Jiang X-J, Zhang X-Z, Li X-Y, Zhang J-F, Zheng Z-B, Zhuo R, Jiang H, Huang C (2009) Novel thermosensitive hydrogel injection inhibits post-infarct ventricle remodelling. European Journal of Heart Failure 11: 14-19.

26. Rane AA, Chuang JS, Shah A, Hu DP, Dalton ND, Gu Y, Peterson KL, Omens JH, Christman KL (2011) Increased Infarct Wall Thickness by a Bio-Inert Material Is Insufficient to Prevent Negative Left Ventricular Remodeling after Myocardial Infarction. PLoS ONE 6: e21571.

27. Huang NF, Yu J, Sievers R, Li S, Lee RJ (2005) Injectable biopolymers enhance angiogenesis after myocardial infarction. Tissue Eng 11: 1860-1866.

28. Lee KY, Mooney DJ (2001) Hydrogels for Tissue Engineering. Chemical Reviews 101: 1869-1880.

29. Callegari A, Bollini S, Iop L, Chiavegato A, Torregrossa G, Pozzobon M, Gerosa G, De Coppi P, Elvassore N, Sartore S (2007) Neovascularization induced by porous collagen scaffold implanted on intact and cryoinjured rat hearts. Biomaterials 28: 5449-5461.

30. Dai W, Wold LE, Dow JS, Kloner RA (2005) Thickening of the infarcted wall by collagen injection improves left ventricular function in rats: a novel approach to preserve cardiac function after myocardial infarction. J Am Coll Cardiol 46: 714-719.

31. Christman KL, Fok HH, Sievers RE, Fang Q, Lee RJ (2004) Fibrin glue alone and skeletal myoblasts in a fibrin scaffold preserve cardiac function after myocardial infarction. Tissue Eng 10: 403-409.

32. Landa N, Miller L, Feinberg MS, Holbova R, Shachar M, Freeman I, Cohen S, Leor J (2008) Effect of injectable alginate implant on cardiac remodeling and function after recent and old infarcts in rat. Circulation 117: 1388-1396.

33. Leor J, Tuvia S, Guetta V, Manczur F, Castel D, Willenz U, Petnehazy O, Landa N, Feinberg MS, Konen E, Goitein O, Tsur-Gang O, Shaul M, Klapper L, Cohen S (2009) Intracoronary injection of in situ forming alginate hydrogel reverses left ventricular remodeling after myocardial infarction in Swine. J Am Coll Cardiol 54: 1014-1023.

34. Ou L, Li W, Zhang Y, Wang W, Liu J, Sorg H, Furlani D, Gabel R, Mark P, Klopsch C, Wang L, Lutzow K, Lendlein A, Wagner K, Klee D, Liebold A, Li RK, Kong D, Steinhoff G, Ma N (2011) Intracardiac injection of matrigel induces stem cell recruitment and improves cardiac functions in a rat myocardial infarction model. J Cell Mol Med 15: 1310-1318.

35. Albini A, Melchiori A, Garofalo A, Noonan DM, Basolo F, Taraboletti G, Chader GJ, Gavazzi R (1992) Matrigel promotes retinoblastoma cell growth in vitro and in vivo. Int J Cancer 52: 234-240.

36. Crapo PM, Gilbert TW, Badylak SF (2011) An overview of tissue and whole organ decellularization processes. Biomaterials 32: 3233-3243.

37. Kochupura PV, Azeloglu EU, Kelly DJ, Doronin SV, Badylak SF, Krukenkamp IB, Cohen IS, Gaudette GR (2005) Tissue-engineered myocardial patch derived from extracellular matrix provides regional mechanical function. Circulation 112: I144-149.

38. Freytes DO, Martin J, Velankar SS, Lee AS, Badylak SF (2008) Preparation and rheological characterization of a gel form of the porcine urinary bladder matrix. Biomaterials 29: 1630-1637.

39. Robinson KA, Li JS, Mathison M, Redkar A, Cui JH, Chronos NAF, Matheny RG, Badylak SF (2005) Extracellular matrix scaffold for cardiac repair. Circulation 112: I135-I143.

40. Zhao ZQ, Puskas JD, Xu D, Wang NP, Mosunjac M, Guyton RA, Vinten-Johansen J, Matheny R (2010) Improvement in Cardiac Function With Small Intestine Extracellular Matrix Is Associated With Recruitment of C-Kit Cells, Myofibroblasts, and Macrophages After Myocardial Infarction. Journal of the American College of Cardiology 55: 1250-1261.

41. Laflamme MA, Murry CE (2005) Regenerating the heart. Nat Biotechnol 23: 845-856.

42. Christman KL, Vardanian AJ, Fang Q, Sievers RE, Fok HH, Lee RJ (2004) Injectable fibrin scaffold improves cell transplant survival, reduces infarct

expansion, and induces neovasculature formation in ischemic myocardium. J Am Coll Cardiol 44: 654-660.

43. Lu WN, Lu SH, Wang HB, Li DX, Duan CM, Liu ZQ, Hao T, He WJ, Xu B, Fu Q, Song YC, Xie XH, Wang CY (2009) Functional improvement of infarcted heart by co-injection of embryonic stem cells with temperature-responsive chitosan hydrogel. Tissue Eng Part A 15: 1437-1447.

44. Christman KL, Singelyn JM, Salvatore M, Schup-Magoffin PJ, Hu DP, Johnson T, Bartels K, DeMaria AN, Dib N (2011) CATHETER-DELIVERABLE HYDROGEL DERIVED FROM DECELLULARIZED VENTRICULAR EXTRACELLULAR MATRIX INCREASES CARDIOMYOCYTE SURVIVAL AND PRESERVES CARDIAC FUNCTION POST-MYOCARDIAL INFARCTION. J Am Coll Cardiol 57: E2017-.

45. Singelyn JM, Christman KL (2011) Modulation of material properties of a decellularized myocardial matrix scaffold. Macromol Biosci 11: 731-738.

46. DeQuach JA, Mezzano V, Miglani A, Lange S, Keller GM, Sheikh F, Christman KL (2010) Simple and high yielding method for preparing tissue specific extracellular matrix coatings for cell culture. PLoS ONE 5: e13039.

47. Elliott JT, Tona A, Woodward JT, Jones PL, Plant AL (2002) Thin Films of Collagen Affect Smooth Muscle Cell Morphology†. Langmuir 19: 1506-1514.

48. Flemming RG, Murphy CJ, Abrams GA, Goodman SL, Nealey PF (1999) Effects of synthetic micro- and nano-structured surfaces on cell behavior. Biomaterials 20: 573-588.

49. Koochekpour S, Merzak A, Pilkington GJ (1995) Extracellular matrix proteins inhibit proliferation, upregulate migration and induce morphological changes in human glioma cell lines. Eur J Cancer 31A: 375-380.

50. Silver FH, Freeman JW, Seehra GP (2003) Collagen self-assembly and the development of tendon mechanical properties. J Biomech 36: 1529-1553.

51. Williams BR, Gelman RA, Poppke DC, Piez KA (1978) Collagen fibril formation. Optimal in vitro conditions and preliminary kinetic results. J Biol Chem 253: 6578-6585.

52. Rosenblatt J, Devereux B, Wallace DG (1994) Injectable Collagen as a Ph-Sensitive Hydrogel. Biomaterials 15: 985-995.

53. Hayashi T, Nagai Y (1974) Factors affecting the interactions of collagen molecules as observed by in vitro fibril formation. III. Non-helical regions of the collagen molecules. J Biochem 76: 177-186.

54. Gobeaux F, Mosser G, Anglo A, Panine P, Davidson P, Giraud-Guille MM, Belamie E (2008) Fibrillogenesis in dense collagen solutions: a physicochemical study. J Mol Biol 376: 1509-1522.

55. Bradshaw AD, Baicu CF, Rentz TJ, Van Laer AO, Bonnema DD, Zile MR (2010) Age-dependent alterations in fibrillar collagen content and myocardial diastolic function: role of SPARC in post-synthetic procollagen processing. Am J Physiol Heart Circ Physiol 298: H614-622.

56. Flynn LE (2010) The use of decellularized adipose tissue to provide an inductive microenvironment for the adipogenic differentiation of human adipose-derived stem cells. Biomaterials 31: 4715-4724.

57. Lutolf MP, Hubbell JA (2003) Synthesis and physicochemical characterization of end-linked poly(ethylene glycol)-co-peptide hydrogels formed by Michael-type addition. Biomacromolecules 4: 713-722.

58. Johnson TD, Lin SY, Christman KL (2011) Tailoring material properties of a nanofibrous extracellular matrix derived hydrogel. Nanotechnology 22: 494015.

59. Chan RW, Titze IR (1998) Viscosities of implantable biomaterials in vocal fold augmentation surgery. Laryngoscope 108: 725-731.

60. Leikin S, Rau DC, Parsegian VA (1995) Temperature-favoured assembly of collagen is driven by hydrophilic not hydrophobic interactions. Nat Struct Mol Biol 2: 205-210.

61. Tibbitt MW, Anseth KS (2009) Hydrogels as extracellular matrix mimics for 3D cell culture. Biotechnology and Bioengineering 103: 655-663.

62. Petersen OW, Ronnov-Jessen L, Howlett AR, Bissell MJ (1992) Interaction with basement membrane serves to rapidly distinguish growth and differentiation pattern of normal and malignant human breast epithelial cells. Proc Natl Acad Sci U S A 89: 9064-9068.

63. Engler AJ, Sen S, Sweeney HL, Discher DE (2006) Matrix elasticity directs stem cell lineage specification. Cell 126: 677-689.

64. Miller RR, McDevitt CA (1991) A quantitative microwell assay for chondrocyte cell adhesion. Anal Biochem 192: 380-383.

65. Schubert D, LaCorbiere M (1980) A role of secreted glycosaminoglycans in cell-substratum adhesion. J Biol Chem 255: 11564-11569.

66. Wight TN, Kinsella MG, Qwarnstrom EE (1992) The role of proteoglycans in cell adhesion, migration and proliferation. Curr Opin Cell Biol 4: 793-801.

67. Benitz WE, Kelley RT, Anderson CM, Lorant DE, Bernfield M (1990) Endothelial heparan sulfate proteoglycan. I. Inhibitory effects on smooth muscle cell proliferation. Am J Respir Cell Mol Biol 2: 13-24.

68. Castellot JJ, Jr. (1990) Heparan sulfates: physiologic regulators of smooth muscle cell proliferation? Am J Respir Cell Mol Biol 2: 11-12.

69. Bingley JA, Hayward IP, Campbell JH, Campbell GR (1998) Arterial heparan sulfate proteoglycans inhibit vascular smooth muscle cell proliferation and phenotype change in vitro and neointimal formation in vivo. J Vasc Surg 28: 308-318.

70. Volker W, Bohm A, Schmidt A, Svahn CM, Gellerbring AK, Mattsson C, Ekvarn S, Robenek H, Buddecke E (1995) Inhibition of smooth muscle cell proliferation and neointimal growth by low-anticoagulant heparin. Arzneimittelforschung 45: 546-550.

71. Au YP, Kenagy RD, Clowes MM, Clowes AW (1993) Mechanisms of inhibition by heparin of vascular smooth muscle cell proliferation and migration. Haemostasis 23 Suppl 1: 177-182.

72. Clowes AW, Clowes MM (1989) Inhibition of smooth muscle cell proliferation by heparin molecules. Transplant Proc 21: 3700-3701.

73. Garg HG, Joseph PA, Thompson BT, Hales CA, Toida T, Imanari T, Capila I, Linhardt RJ (1999) Effect of fully sulfated glycosaminoglycans on pulmonary artery smooth muscle cell proliferation. Arch Biochem Biophys 371: 228-233.

74. Thomas DP, McCormick RJ, Zimmerman SD, Vadlamudi RK, Gosselin LE (1992) Aging- and training-induced alterations in collagen characteristics of rat left ventricle and papillary muscle. Am J Physiol 263: H778-783.